Table of Contents

Abstract

A total of twenty 0-20cm soil samples from the El Yunque National Forest, Puerto Rico, have been analyzed using XRD analysis to determine their mineral content. Qualitative and quantitative analysis of the data show that all the samples contain quartz, orthoclase, kaolinite, dickite, halloysite and nicrite, gibbsite, augelite, metavariscite, goethite, tsaregorodtsevite, apophylite. Soil sample from Oxisols sites contain higher percentage of clay minerals than the samples from Dystrudepts sites. Furthermore, the general pattern of the percentage of total clays, feldspars, and gibbsite within each and between transects suggest that soils in the valleys are more weathered and leached than soils from ridges. The percentage increase of phosphate minerals in the soils follow that of clay minerals which is most probably due to the attachment of the phosphate minerals to clay mineral surfaces. The presence of the organic cation Tetramethylammonium in the cavities between the oxygen-silicon tetrahedra of the tsaregorodtsevite structure (feldsphoid-zeolitic structure) is consistent with a low energy mechanism for the sequestration of carbon and nitrogen in the EYNF soils.

Introduction

Soil is the very thin outer skin of the earth's crust that is exploited by plant roots for anchorage and supply of water and nutrients. Soils are developed through the interaction of biology (plants, animals, microbes, and humans), climate (temperature and precipitation), topography (location within a landscape), time and parent material. Soils in the same climate may differ significantly in their mineral content depending on their parent material (Breemen, Buurman, 2002).

Generally, soil form by chemical weathering of rocks at the earth's surface. The byproduct of this weathering process results in solutes (dissolved substances) and secondary minerals typical of soils. These secondary minerals, together with highly resistant primary minerals such as quartz, form the typical minerals of soils.

In this study, samples were collected from soils which are underlain by silicate bedrock. In the following paragraphs I will provide a brief account of the common mineral reactions occurring during the chemical weathering of silicate minerals, the formation of clay minerals and hydroxides, and the interaction between soil minerals and shallow groundwater. (H. Blatt, R. J. Tracy, B. E. Owens, B. E., 2006)

$$\underset{\text{orthoclase}}{3\ KAlSi_3O_8} + 2\ H^+ + 12\ H_2O \rightarrow \underset{\text{muscovite}}{KAl_3SiO_{10}(OH)_2} + \underset{\text{dissolved silica}}{6\ H_4SiO_4^0} + 2\ K^+$$

$$\underset{\text{muscovite}}{2\ KAl_3SiO_{10}(OH)_2} + 2\ H^+ + 3\ H_2O \rightarrow \underset{\text{kaolinite}}{3\ AlSi_2O_5(OH)_2} + 2\ K^+$$

$$\underset{\text{kaolinite}}{AlSi_2O_5(OH)_2} + 5\ H_2O \rightarrow \underset{\text{gibbsite}}{2\ Al(OH)_3} + 2\ H_4SiO_4^0$$

$$\underset{\text{orthoclase}}{2\ KAlSi_3O_8} + 2\ H^+ + 9\ H_2O \rightarrow \underset{\text{kaolinite}}{AlSi_2O_5(OH)_2} + \underset{\text{dissolved silica}}{4\ H_4SiO_4^0} + 2\ K^+$$

$$\underset{\text{muscovite}}{KAl_3SiO_{10}(OH)_2} + H^+ + 9\ H_2O \rightarrow \underset{\text{gibbsite}}{3\ Al(OH)_3} + \underset{\text{dissolved silica}}{3\ H_4SiO_4^0} + K^+$$

$NaAlSi_3O_8 \cdot CaAl_2Si_2O_8 + H_2O + H^+ \rightarrow$

Plagioclase

Na-montmorillonite and/or Ca-montmorillonite + $H_4SiO_4^0$ + $\begin{matrix} Na^+ \\ Ca^{2+} \end{matrix}$

dissolved silica

Ferromagnesian minerals + $H_2O + H^+ \rightarrow$

Na-montmorillonite and/or Ca-montmorillonite and/or kaolinite and/or gibbsite + $H_4SiO_4^0$ + $Fe(OH)_3$

dissolved silica; freeic hydroxide

$2\ Fe(OH)_3 \rightarrow Fe_2O_3 + 3\ H_2O$ or $Fe(OH)_3 \rightarrow FeO(OH) + 3\ H_2O$

ferric hydroxide; hematite — ferric hydroxide; goethite

What of a note here is that although the above reactions seem straight forward and precise in the way they are written, in reality these reactions are more complex and less precise. However, two generalizations can be made: 1) Reaction products contain less silica and smaller proportion of metallic cations than the input minerals; 2) As temperature and precipitation increase, the stable reaction products, such as Kaolinite, gibbsite, and goethite, become increasingly less complex; under the most intense humid tropical conditions, simple aluminous gibbsite and ferric compounds, like hematite and goethite, (crystalline or amorphous) are likely to be the only things that remain (H. Blatt, R. J. Tracy, and B. E. Owens, 2006).

From the above, it is clear that the characterization of soils mineral content can aid in an improved understanding of the physical and chemical differences between soils. In particular the qualitative and quantitative analysis of clay minerals, gibbsite, feldspars, phosphates, mineralized organic matter present in soils will help determine soil developmental history.

In this study twenty soil samples overlying two different kinds of bedrock were collected from the El Yunque National Forest, Puerto Rico. Samples were analyzed for their mineral content using X-ray diffraction patterns and quantitative Rietveld analysis to address the following questions:

1. Are there significantly differences between the clay mineralogy of soils overlying the two different?

2. Are there differences in the % of total clay, feldspars, and gibbsite within each and between rock types and topographic position?

3. Are these differences in the mineralogy that indicates differences in the degree and extent of weathering?

4. To investigate the presence or absence of non-silicate minerals which could influence the nutrient pool of the soil?

Chapter I will provide the geology description of the El Yunque National Forest of Puerto Rico. Also the general climate information will be introduced. Chapter II is the method used in this study including the fieldwork, laboratory, and the analysis method. Chapter III introduces the background of clay minerals and the polymorphism in kaolin group. Chapter IV describes the result from the analysis: the general mineral present in the samples and the detail about the clay-gibbsite-feldspar association, the Tsaregorodtsevite which contents organic cation, and the phosphate minerals following by a conclusion.

Chapter I

Description of the tropical forest of Puerto Rico

1.1 Geologic setting of the study area

Puerto Rico is located between the Caribbean Sea and the Atlantic Ocean and consists of the main island of Puerto Rico and various smaller islands (Fig. 1). In the following paragraphs I will present a brief account about the general geologic setting of the island, description of its major tropical forest and the major climatic variables affecting the island.

Puerto Rico is at the eastern end of the Greater Antilles island arc, which was active volcanically from late Jurassic or early Cretaceous (Maastrichtian, about 65-73 Ma) until Eocene time (56 to 34 Ma) (Kesler, S.E., Sutter, J.F., 1979). Volcaniclastic rocks are marine-deposited volcanic ash, which are related to a wide spectrum of eruptive and sedimentary mechanisms, and occur close to regions with subaerial and submarine active volcanism. Development of a stable platform in the Oligocene (34 Ma to 23 Ma) allowed for the deposition of clastic volcanic matrial and carbonate sequences at this island. Volcaniclastic rocks in the survey area vary in appearance, but because they are derived from the same pool of magma they have essentially the same mineralogical composition. These rocks are predominantly composed of basic feldspars and smaller amounts of ferromagnesian minerals, which weather to a soil high in iron and aluminum oxide clay but low in silica and free base (USDA, 2001, Figure 2).

In Puerto Rico, intrusive rocks of significant size developed during the later phases of volcanic activity in late Cretaceous and early Cenozoic time (Kesler, S.E., Sutter, J.F., 1979). The quartz diorites, the intrusive rocks in the survey area, are light-gray, medium to coarse-grained rocks. The typical mineral composition of this rock is about 26 percent quartz, 5 percent orthoclase, 59 percent plagioclase, 6 percent hornblende, and 4 percent biotite (Leyrit, Montenat, 2000).

Figure 1. Regional location (right side) and elevation information of the island Puerto Rico

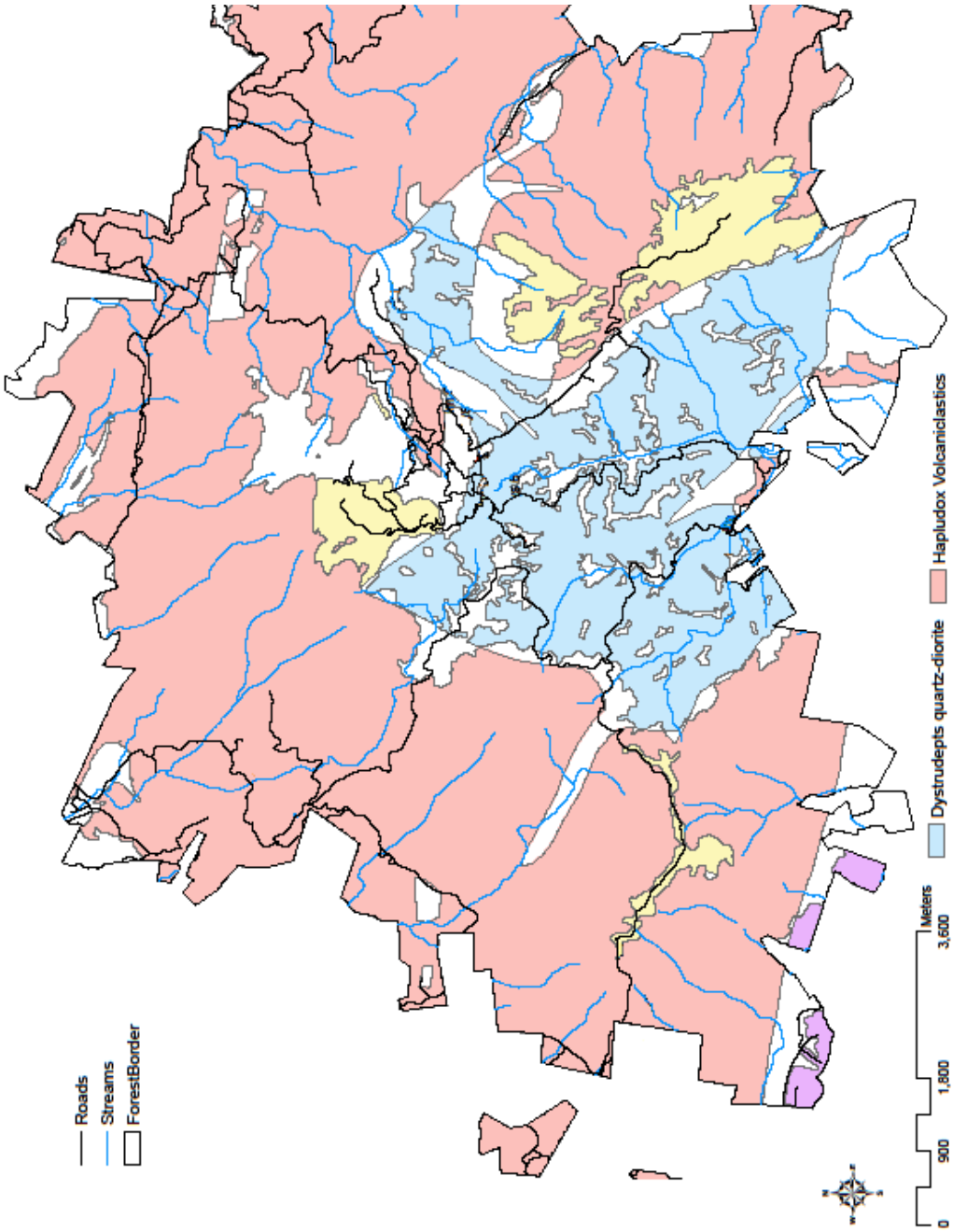

Figure 2. Two major bedrock types in the EYNF, Puerto Rico

The substantial amount of quartz in the quartz diorite accumulates residually during the weathering process because quartz resists decomposition (USDA, 1999).

1.2 The El Yunque National Forest

The El Yunque National Forest (EYNF), also known as the Luquillo Experimental Forest, includes 28,000 acres of tropical forest in northeastern Puerto Rico (Figure 3). The EYNF is an area of high relief with elevations ranging from 200 to 1300 m. The topography is rugged and the slopes are highly dissected. Slopes range from 10 to 100 percent (USDA, 2001). El Yunque is the only tropical rain forest in the United States National Forest System (US Forest Service, 2009).

There are four main forest types in the EYNF: Tabonuco, Palo Colorado, Sierra Palma and Dwarf (Figure. 4). All samples are collected from Tabonuco, Palm, and Colorado forest. No sample is collected from the Dwarf forest. The tabonuco forest is named for the dominant tabonuco tree that covers the lower forst slopes to about 600 m in elevation. The palo colorado forest, named for the palo colorado tree, begins above the tabonuco forest and extends up to about 900 m. At the same elevation with colorado and tabonuco forests, but in mostly steep and wet areas, is palm forest, heavily dominated by the sierra palm. This forest type may indicate unstable soils. (USDA, 2001)

1.3 Distribution of Temperature and Precipitation

Located in the tropics, Puerto Rico has an average temperature of 27 °C (80.6 °F) throughout the year. The seasons do not change very drastically. The temperature in the south is usually a few degrees higher than in the north and temperatures and the central interior mountains are always cooler than the rest of the island. The dry season spans from November to May while the wet season coincides with the Atlantic hurricane season from June to November (McKnight, 2000).

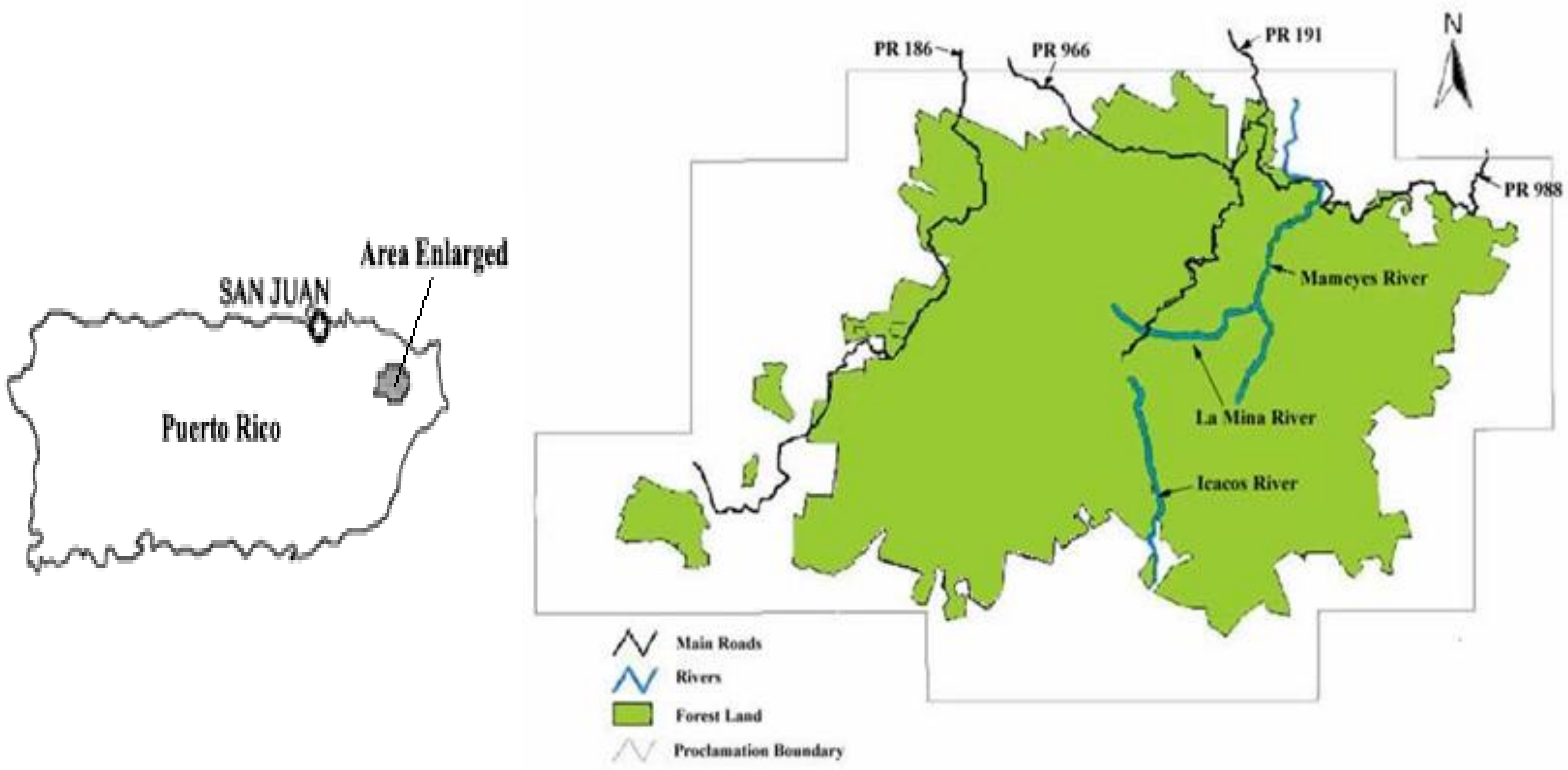

Figure 3. Location of the El Yunque National Forest (EYNF) in the island Puerto Rico

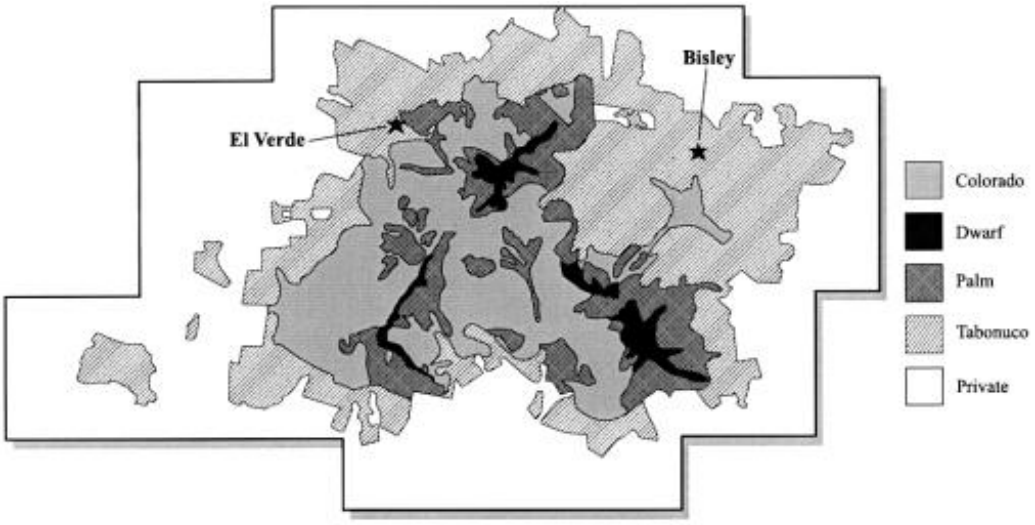

Figure 4. The four major forest types in the EYNF

For the EYNF, the mean annual precipitation reaches as high as 450 cm with an average of 230 cm per year. The temperature decreases as elevation and rainfall increase. The highest locations are also the coolest with mean annual temperatures (MAT) of 21 to 20°C.

1.4 Soil types in the El Yunque National Forest

In the EYNF, intense, continuous weathering in the warm, humid tropical climate has transformed the rocks into saprolite. The highly leached soils formed from the saprolite are classified as Oxisols (Ox in sample name), Ultisols, and Inceptisols. Because the lithology of the country rock determines the quartz and clay content of the saprolite, the soils in the area of volcaniclastic rocks are clayey and the soils in the quartz diorite area are sandy or loamy, but still contain significant amount of clay. Much of the soil formed on the quartz-diorite parent material in the EYNF is defined as Dystrudepts (Dys in sample name, a suborder of the Inceptisols). The soil collected from the Volcaniclastic rocks area is Oxisols. Also, Eutrudepts (the more or less freely drained Inceptisols) and Endoaquepts (wet Inceptisols) are present in the EYNF. (Figure 5)

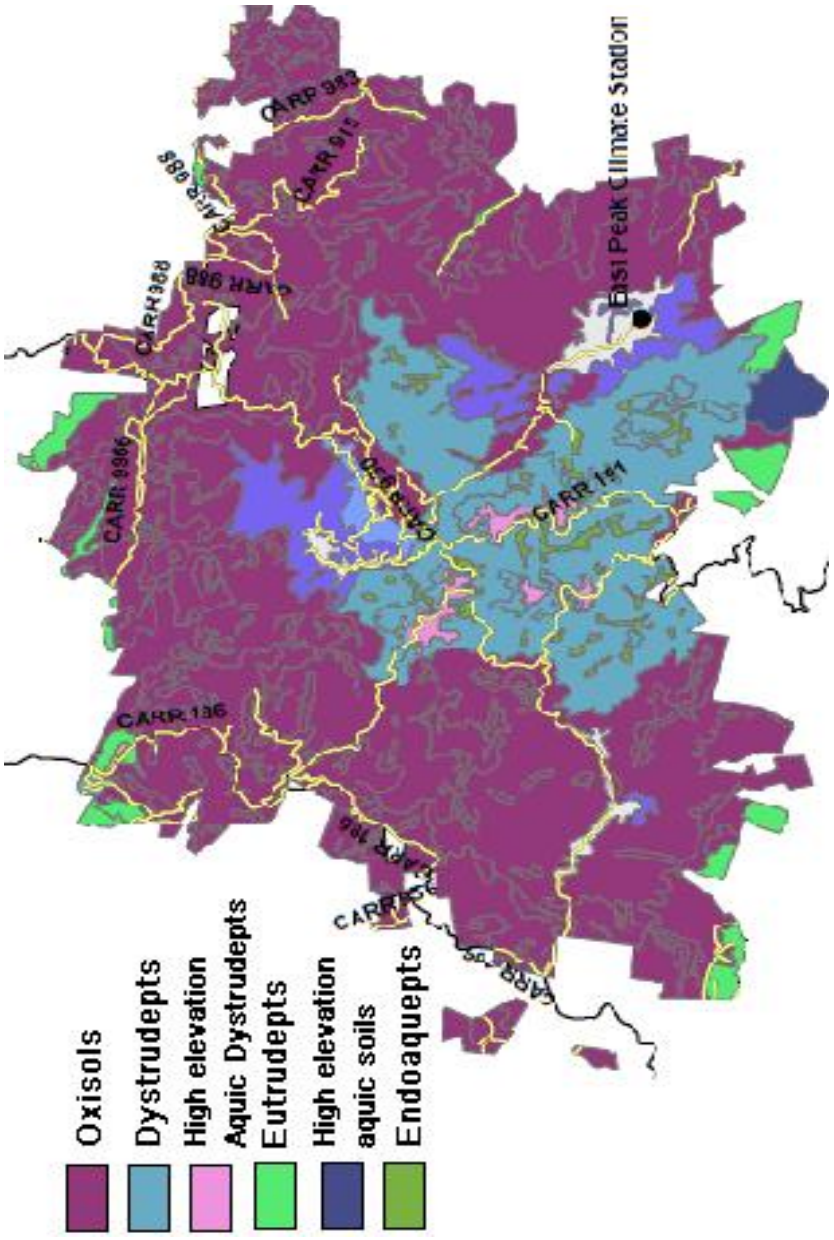

Figure 5. The six major soil groups in the EYNF

Chapter II

Field and laboratory work

In the summer of 2010, supervised by John Clark, twenty sites along ten transects were sampled from the EYNF based on soil type and vegetation. (Figure 6 A, B) The higher elevation samples are designated with R (ridge) and lower elevation samples are designated with V (valley). The relief varies with different transect between ridge and valley at the range from 3 to 45m. Soil types reflect the two different parent materials: volcaniclastic rocks and quartz-diorites. Three different forest types reflect the different range of elevations related to the change of climate. Using the quantitative pit method, pits were excavated by first securing a 25 × 25 cm frame (inside area) with long nails and removing all live vegetation and dead wood. Forest floor material was collected from within the square and placed in a separate bag for processing. A 20 cm deep block of mineral soil was then carefully excavated. Roots were manually removed in the field.

In the laboratory, soils were air-dried and passed through a 2 mm sieve prior to analyses. For the X-ray diffraction (XRD) examination, two sample preparation protocols have been employed: 1) a few grams of <2mm fraction of the whole sample was ground in ball-mill to a size of ~10 microns, 2) clays were separated from the coarse fraction (sand and gravel) and silt by settling using the Bouyoucos Method (Gee, Bauder 1986) and following the Laboratory Manual from USGS open file Report 01-041. For the purpose of getting the original result for all samples for future comparison, chemical treatment (hydrogen peroxide treatment to remove organics, dithionite-citrated system buffered with sodium bicarbonate to remove iron oxide) was only applied on one sample.

To see how organic matter and Fe-oxides in the samples analyzed affect the clarity of the XRD patterns of these samples, Col Ox 1-4 clay-size fraction was treated by hydrogen peroxide to remove organic matter and dithionite-citrated system buffered with sodium bicarbonate to remove iron oxide. With one exception, the XRD pattern of the treated sample shows no noticeable difference (as to the number of peaks and the clarity) in comparison to the pattern of the untreated sample. The one exception is a

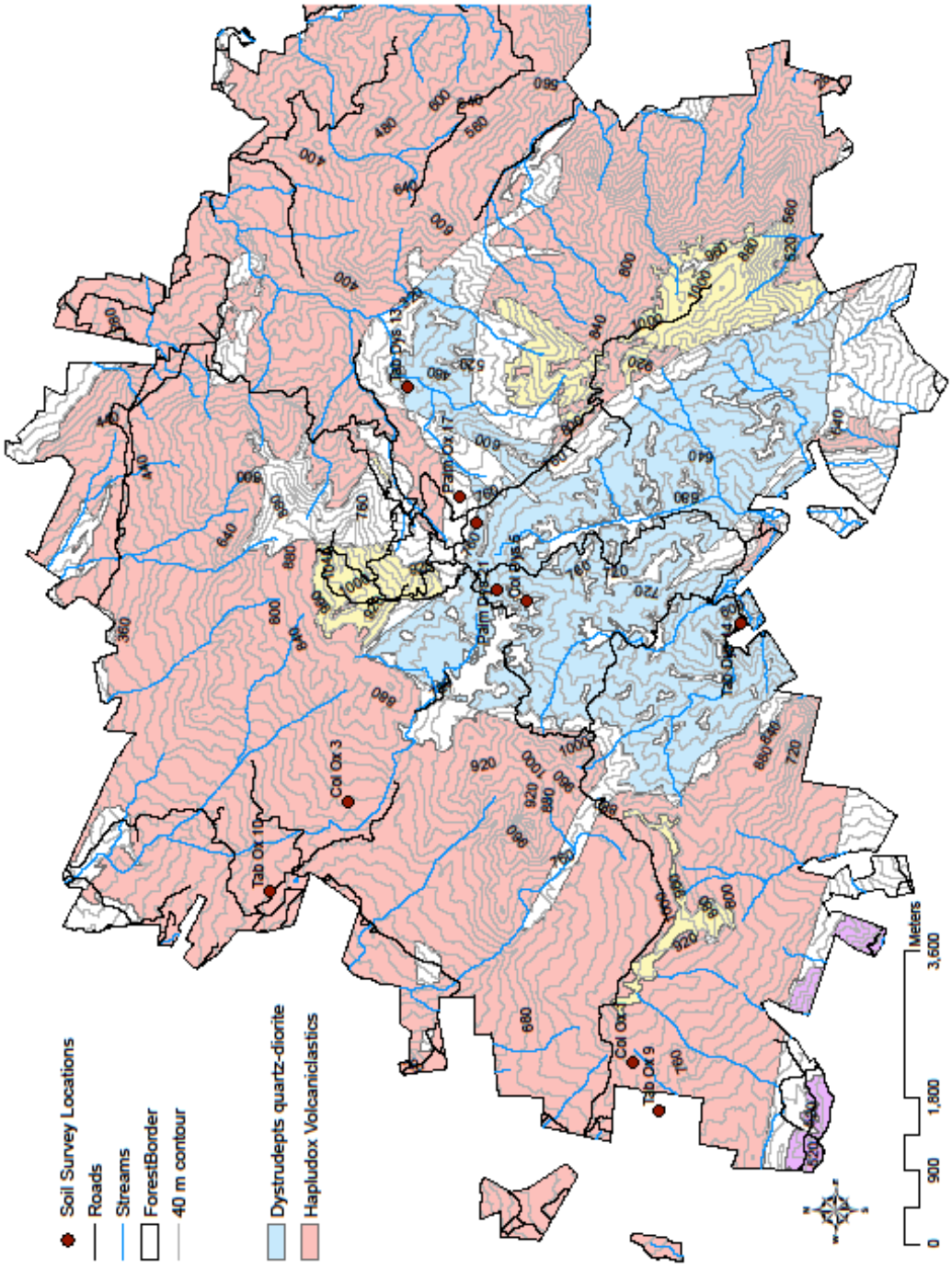

Figure 6A. Samples locations in the EYNF

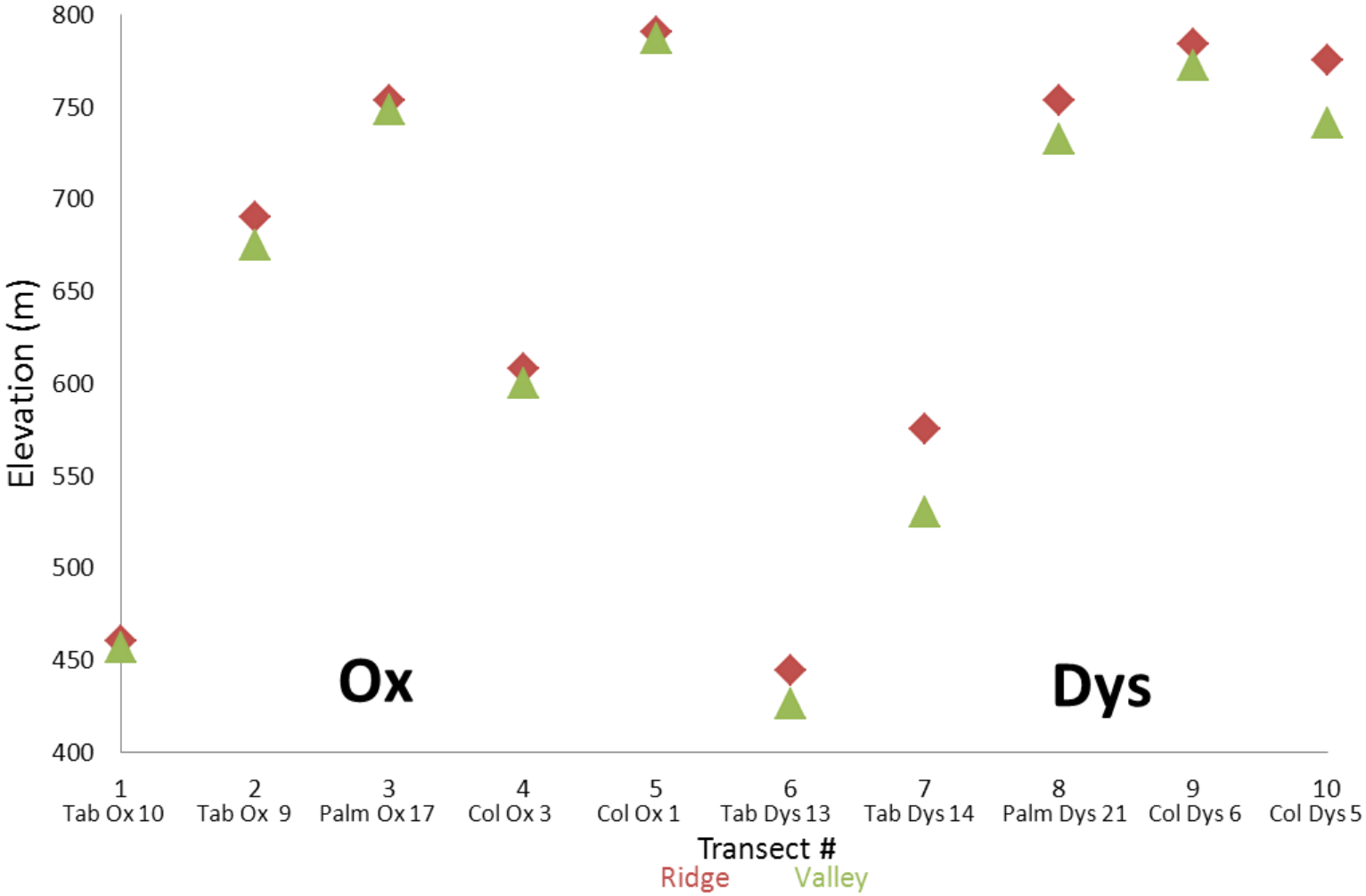

Figure 6B. Elevation of samples used in this study

missing peak at 14.1° in the XRD profile of the treated sample which identified as belonging to the mineral Tsargeordodtesvite.

The powder of 30 whole samples and 30 clay-size fractions were mounted in the sample holders. Samples were analyzed by X-ray diffraction in a Pananalytical X'Pert Pro instrument. Samples were scanned using copper tube (λ 1.54055 Å) at a step size of 0.017° between 5.00 and 75.00° (2θ). The samples were rotated during measurement for 1.5 hours each. Divergence slit of ½° and anti-scatter slit of 1° were used.

X' Pert HighScore Plus, version 2.2 (2.2.0), was used to provide a list of the possible minerals that best fit the peaks (peak's position, height, and width) in the XRD patterns obtained for each sample. Quantitative analysis for each sample was carried out using Rietveld analysis. Rietveld analysis (Maud), version 1.993, is based on the construction of a calculated XRD pattern that is based on the atomic structure of minerals. The most important feature of this analysis is that it takes into account the overlapping of peaks; a problem which cannot be detected by highscore software. A best fit between the observed and calculated XRD pattern was obtained by adding and subtracting potential possible minerals. After the best possible fit is obtained, the percentage of each mineral is calculated.

What of a note here is that because the amount of quartz in whole sample is high to the extent, which it drastically decrease the height of the peaks of other minerals present in the whole soil sample. This effect will make the identification and quantification of minerals (particularly of clays) very difficult and even if achieved the results will be highly uncertain. To remedy this situation the whole soil samples were process to obtain the clay-size fraction with the aim of amplifying the XRD signal of all the minerals present in the sample except quartz.

Chapter III

Polymorphism in kaolinite

Clay minerals are the weathering products of silicate minerals. These are by far the most important secondary minerals in tropical soils. Because clay minerals have a large surface area and have charged surfaces, consequently have high cation exchange capacity, these minerals can strongly influence many soil characteristics. Silicate clays, aluminum and iron oxides and very resistant weathering products and are the three main groups of minerals found in highly weathered soils.

The crystal structure of clay is a sheeted-layer structure with strong bonding (covalent) within each sheet, but weak bonding between the adjacent two- or three-sheet layers. The week bonding between layers permits the adsorption of metallic cations and organic substances on clay mineral surfaces. The clay mineral structure contains two types of sheets. The first type is a tetrahedral sheet (Figure 7) composed of tetrahedrally coordinated Si-O and Al-O groups in which three of the four oxygen atoms share with adjoining groups. The second sheet type is an octahedral sheet (Figure 7) composed of Al-OH or Mg-OH groups in octahedral coordination (Klein, Dutrow, 2007).

Silicate clays can be classed into 1:1 structure, 2:1 structure and 2:1:1 structure based on the nature of their sheeting pattern. Kaolin minerals are dioctahedral clays of 1:1 layer type with chemical composition $Al_2Si_2O_5(OH)_4$. Members of kaolin mineral group include kaolinite and its polymorphs dickite, nacrite, and halloysite.

The kaolinite stacking sequence consists of identical layers with an interlayer shift of –a/3. In well-crystalized kaolinite each layer is identical and has octahedral site (C or B) vacant. (Figure 8, Cruz) Kaolinite has a one-layer monoclinic (1M) structure with **β**= 104 and space group Cm.

The polymorphs of kaolinite differ in terms of two factors: 1) the direction and

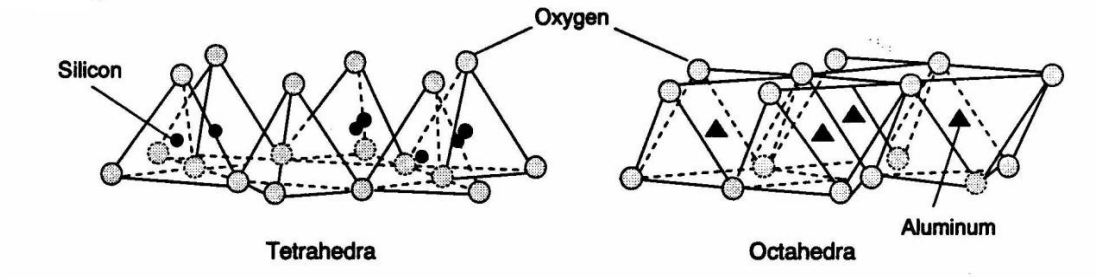

Figure 7. The structure of tetrahedron sheet and octahedron sheet in clay minerals (Klein, Dutrow, 2007)

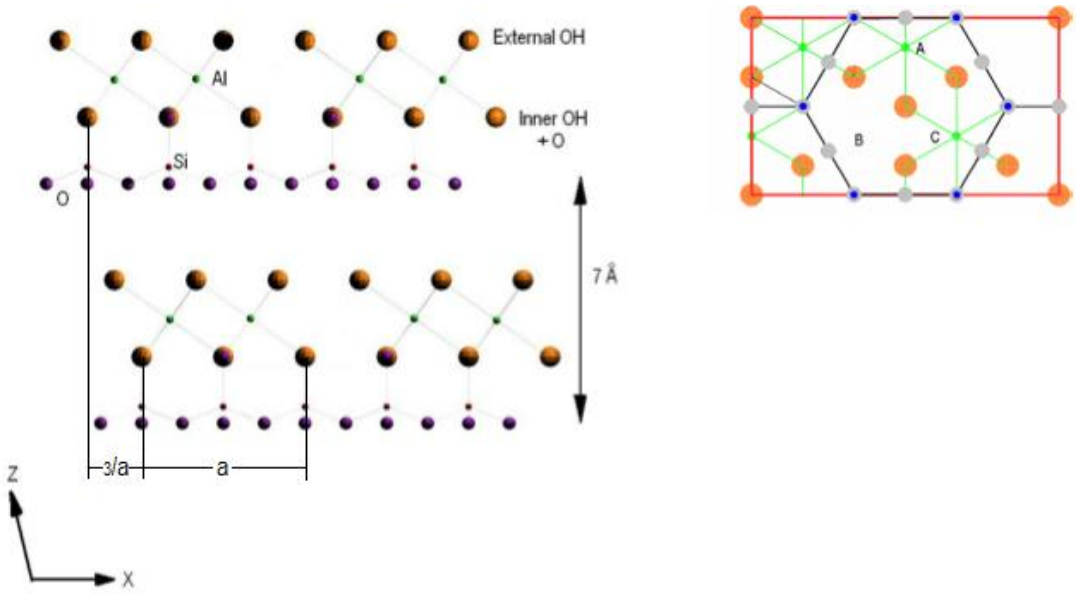

Figure 8. Left: [010] view of the elemental structure of the kaolin group minerals

Right: Types of octahedral site vacant. (Bailey, 1963)

amount of the interlayer shift, and 2) the location of the vacant octahedral site in successive layers. (Murray, 1988)

In dickite the vacant site of the octahedral sheet alternates between two distinct sites (C and B, Figure 9). The alternations of vacant site between B and C in successive layers create a two-layer stacking sequence and change the space group to Cc (one of the low temperature, low symmetry forms). The interlayer shift is also –a/3.

Nacrite has two-layer stacking sequence, as dickite, with **β** values of approximately 100 and 114. The interlayer shift is slightly greater than a/3 pre layer. The space group is Cc.

Halloysite is a hydrated polymorph of kaolinite with curved layers and a spacing of 10Å when fully hydrated; the spacing decreases to 7 Å upon dehydration.

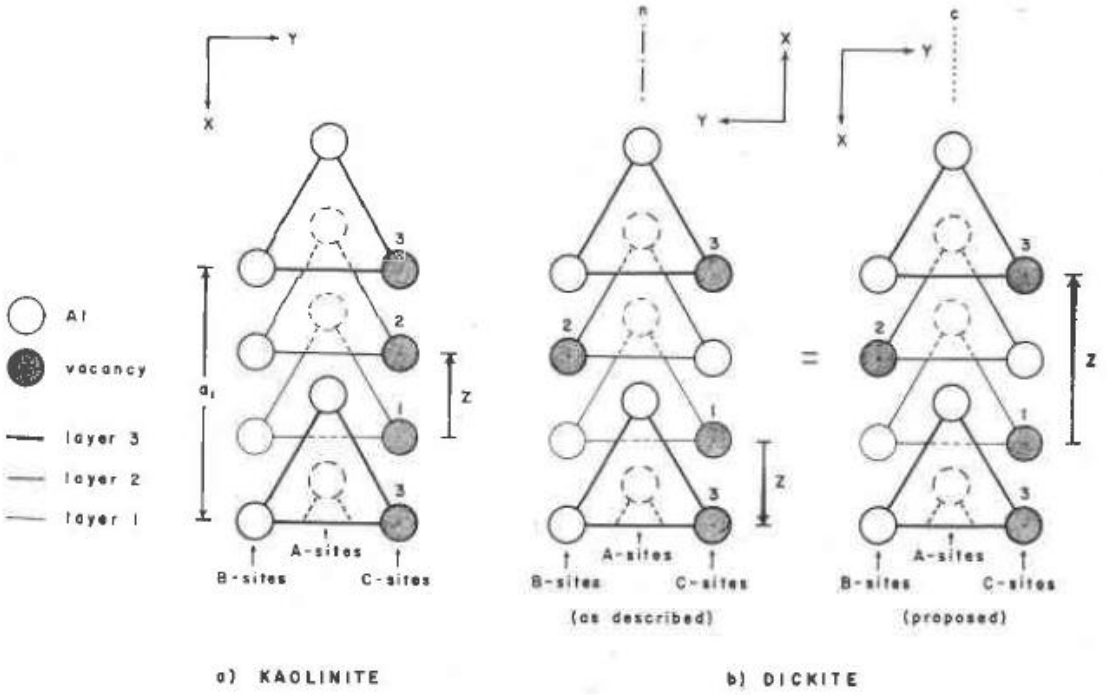

Figure 9. Three views projected onto (001) of the octahedral sites in kaolinite and dickite showing the possible placement of the vacant octahedral site. In each of these views the X direction is down and the Y direction is across from left to right. (Bailey, 1963)

Chapter IV

Result and Discussion

The qualitative XRD analysis indicates the presence of the following minerals in the whole samples and the clay-size fractions: quartz, orthoclase, clay minerals (kaolinite, dickite, halloysite and nicrite), gibbsite, phosphate (augelite and metavariscite), goethite, tsaregorodtsevite, apophylite. Albite, melsnovanadite and vermiculite only present at samples from Dystrudepts sites. (Table 1, 2)

The amount of quartz presence whole soil sample varies with bedrocks with the difference between 13.67% Col Ox 1-4 R to 77.76% Col dys 6-132 V. It's clear that soil sample from Dys sites contain much more quartz than sample from Oxisols. Quartz from the Oxisols sites has the percentage range from 13.67% to 31.16% while the range in Dystrudepts sites is 16.25% to 77.76%. The percentage of quartz shows dramatic drop in clay size fraction which indicates a good result of separation. (Figure 10)

Small amount of apophylite ($KCa_4(Si_4O_{10})_2F{\cdot}8(H_2O)$) presents in most of the samples at range around 0.13% to 2.56%.

Goethite ($FeO(OH)$) present in all samples but Tab Dys 14-165. Its amount changes from as low as 0.74% up to 8.99%. The presence goethite in the analyzed soil samples will cause the scatter of the diffracted x-ray beam that would affect the observation of XRD pattern.

Melanovanadite ($Ca_2V_8O_{20}{\cdot}10H_2O$, P. Bayliss, J.M. Hughes, 1985) is found in some of the Dystrudepts samples by the range from 0.73% to 2.70%.

As mentioned earlier in introduction the mineral association feldspar-clay-gibbsite provides an excellent indicator of the degree and history of the weathering of soils. Therefore, in the following discussion I will discuss the amount of these three minerals obtained in this study in terms of elevation, type of bedrock, the degree and magnitude of weathering of the soils in Puerto Rico.

Table 1. Mineral content of 0-20cm whole soil samples by transects in the EYNF

Transect Code		1				2			
Sample #		Tab Ox 10-28 R		Tab Ox 10-30 V		Tab Ox 9-67 R		Tab Ox 9-69 V	
Elevation (m)		460		457		690		675	
Mineral		%	+/-	%	+/-	%	+/-	%	+/-
Apophylite		2.28	*0.38*	0.98	*0.32*	0.13	*0.16*	2.14	*0.35*
Phosphate	Augelite	4.4	*0.45*	6.64	*0.39*	5.88	*0.43*	4.58	*0.42*
	Metavariscite	5.55	*0.43*	5.24	*0.37*	4.53	*0.39*	3.71	*0.39*
	Σ	9.95	*0.62*	11.88	*0.54*	10.41	*0.58*	8.29	*0.57*
Gibbsite		2.58	*0.35*	2.75	*0.31*	2.08	*0.28*	1.12	*0.3*
Goethite		8.99	*0.27*	7.47	*0.23*	5.58	*0.24*	5.96	*0.24*
Feldspar	Orthhoclase	4.68	*0.5*	5.38	*0.46*	4.34	*0.48*	4.54	*0.49*
	Albite	0	*0*	0	*0*	0	*0*	0	*0*
	Σ	4.68	*0.5*	5.38	*0.46*	4.34	*0.48*	4.54	*0.49*
Clays	Dickite	7.78	*1.09*	9.36	*0.72*	9.03	*0.72*	22.69	*1.68*
	Haolloysite	21.7	*1.1*	12	*0.91*	23	*1.13*	14.44	*1.08*
	Kaolinite	15.36	*1.27*	18.02	*0.94*	19.76	*0.99*	13.92	*1.83*
	Nacrite	10.82	*0.69*	14.31	*1*	9.88	*0.73*	8.46	*0.94*
	Σ	55.66	*2.12*	53.69	*1.8*	61.67	*1.82*	59.51	*2.86*
Quartz		15.24	*0.38*	18.01	*0.35*	13.81	*0.28*	16.45	*0.39*
Tsargorodtsevite		0.62	*0.24*	0	*0*	1.96	*0.21*	1.8	*0.21*
Vermiculite		0	*0*	0	*0*	0	*0*	0	*0*
Melanovanadite		0	*0*	0	*0*	0	*0*	0	*0*
Σ		100	*2.38*	100.16	*2.03*	99.98	*2.04*	99.81	*3.03*

Table 1 Continued

Transect Code		3				4			
Sample #		Palm Ox 17-91 R		Palm Ox 17-93 V		Col Ox 3-61 R		Col Ox 3-63 V	
Elevation (m)		753		748		608		600	
Mineral		%	+/-	%	+/-	%	+/-	%	+/-
Apophylite		1.35	*0.34*	0	*0*	0	*0*	1.6	*0.29*
Phosphate	Augelite	5.91	*0.44*	6.09	*0.42*	7.43	*0.59*	8.23	*0.31*
	Metavariscite	4.76	*0.41*	4.62	*0.42*	5.32	*0.48*	5.74	*0.31*
	Σ	10.67	*0.6*	10.71	*0.59*	12.57	*0.76*	13.97	*0.44*
Gibbsite		3.03	*0.35*	17.41	*0.68*	9.26	*0.8*	19.96	*0.47*
Goethite		5.3	*0.22*	4.77	*0.24*	7.93	*0.29*	5.3	*0.17*
Feldspar	Orthhoclase	4.88	*0.5*	4.01	*0.55*	5.12	*0.73*	2.97	*0.31*
	Albite	0	*0*	0	*0*	0	*0*	0	*0*
	Σ	4.88	*0.5*	4.01	*0.55*	5.12	*0.73*	2.97	*0.31*
Clays	Dickite	8.76	*0.81*	10.16	*0.74*	6.71	*2.43*	8.93	*0.49*
	Haolloysite	21.1	*1.17*	9.46	*0.59*	14.43	*1.92*	8.12	*0.43*
	Kaolinite	9.52	*1.18*	5.49	*0.82*	17.39	*1.56*	12.62	*0.57*
	Nacrite	10.75	*0.84*	6.2	*1.02*	10	*2.98*	11.09	*0.62*
	Σ	50.13	*2.03*	31.52	*1.62*	48.53	*4.57*	40.76	*1.06*
Quartz		24.02	*0.47*	31.16	*0.52*	15.53	*0.6*	14.76	*0.28*
Tsargorodtsevite		0.6	*0.23*	0.4	*0.34*	0.83	*0.24*	0.68	*0.16*
Vermiculite		0	*0*	0	*0*	0	*0*	0	*0*
Melanovanadite		0	*0*	0	*0*	0	*0*	0	*0*
Σ		99.98	*2.3*	99.98	*2.04*	99.77	*4.81*	100	*1.36*

Table 1 Continued

Transect Code		5				6			
Sample #		Col Ox 1-4 R		Col Ox 1-6 V		Tab Dys 13-82 R		Tab Dys 13-84 V	
Elevation (m)		790		787		444		426	
Mineral		%	+/-	%	+/-	%	+/-	%	+/-
Apophylite		0	*0*	0.78	*0.46*	2.56	*0.38*	3.24	*0.42*
Phosphate	Augelite	5.06	*0.5*	5.96	*0.42*	4.24	*0.93*	2.94	*0.4*
	Metavariscite	5.55	*0.46*	3.58	*0.39*	2.59	*0.51*	3.46	*0.39*
	Σ	10.61	*0.68*	9.54	*0.57*	6.83	*1.06*	6.4	*0.56*
Gibbsite		0	*0*	3.43	*0.3*	0.27	*0.44*	17.05	*0.64*
Goethite		8.25	*0.27*	6.52	*0.24*	7.6	*0.35*	6.34	*0.24*
Feldspar	Orthhoclase	0.99	*0.4*	5.61	*0.53*	5.45	*0.54*	1.31	*0.48*
	Albite	0	*0*	0	*0*	2.39	*0.39*	3.5	*0.57*
	Σ	0.99	*0.4*	5.61	*0.53*	7.48	*0.67*	4.81	*0.75*
Clays	Dickite	11.93	*1.09*	14.37	*0.72*	9.28	*1.52*	5.68	*0.69*
	Haolloysite	8.01	*0.8*	15.72	*1.3*	10.41	*1*	6.24	*0.51*
	Kaolinite	22.07	*1.63*	14.05	*0.91*	22.68	*1.48*	10.96	*0.79*
	Nacrite	20.43	*1.09*	12.14	*1.07*	13.32	*1.4*	1.27	*0.61*
	Σ	62.46	*2.38*	56.28	*2.05*	55.69	*2.73*	24.15	*1.32*
Quartz		13.67	*0.31*	15.79	*0.37*	16.25	*0.98*	36.19	*0.57*
Tsargorodtsevite		4.02	*0.29*	2.05	*0.21*	2.95	*0.3*	1.82	*0.3*
Vermiculite		0	*0*	0	*0*	0	*0*	0	*0*
Melanovanadite		0	*0*	0	*0*	0	*0*	0	*0*
Σ		100	*2.56*	100	*2.31*	99.63	*3.25*	100	*1.92*

Table 1 Continued

Transect Code		7				8			
Sample #		Tab Dys 14-163 R		Tab Dys 14-165 V		Palm Dys 21-118 R		Palm Dys 21-120 V	
Elevation (m)		575		530		753		732	
Mineral		%	+/-	%	+/-	%	+/-	%	+/-
Apophylite		1.64	*0.36*	0	*0*	0	*0*	0.67	*0.32*
Phosphate	Augelite	0	*0*	2.56	*0.4*	0.65	*0.33*	0.94	*0.25*
	Metavariscite	2.57	*0.41*	2.43	*0.41*	3.98	*0.41*	3.09	*0.34*
	Σ	2.57	*0.41*	4.99	*0.57*	4.63	*0.53*	4.03	*0.42*
Gibbsite		0.44	*0.28*	0	*0*	2.36	*0.35*	0	*0*
Goethite		0.74	*0.22*	0	*0*	2.53	*0.21*	2.52	*0.19*
Feldspar	Orthhoclase	4.75	*0.71*	6.31	*0.64*	1.77	*0.43*	2.1	*0.29*
	Albite	39.28	*0.99*	34.31	*1.01*	2.08	*0.38*	7.97	*0.36*
	Σ	44.03	*1.12*	40.62	*1.2*	3.85	*0.57*	10.07	*0.46*
Clays	Dickite	0	*0*	0.66	*0.65*	5.48	*0.98*	3.57	*0.69*
	Haolloysite	5.28	*0.55*	3.59	*0.52*	6.4	*0.52*	5.27	*0.43*
	Kaolinite	6.27	*0.99*	4.09	*0.64*	5.35	*0.97*	8.07	*0.84*
	Nacrite	0.53	*0.55*	2	*0.62*	11.27	*1.06*	1.82	*0.32*
	Σ	12.08	*1.26*	10.34	*1.22*	28.5	*1.82*	18.73	*1.21*
Quartz		34.42	*0.61*	41.97	*0.67*	57.42	*0.66*	62.93	*0.59*
Tsargorodtsevite		0	*0*	0	*0*	0.69	*0.26*	0	*0*
Vermiculite		1.35	*0.04*	1.33	*0.05*	0	*0*	0	*0*
Melanovanadite		2.7	*0.26*	0.73	*0.27*	0	*0*	1.03	*0.21*
Σ		99.97	*1.93*	99.98	*1.94*	99.98	*2.14*	99.98	*1.54*

Table 1 Continued

Transect Code		9				10			
Sample #		Col Dys 6-130 R		Col dys 6-132 V		Col Dys 5-79 R		Col Dys 5-81 V	
Elevation (m)		784		772		775		741	
Mineral		%	+/-	%	+/-	%	+/-	%	+/-
Apophylite		0	*0*	0.91	*0.27*	2.02	*0.33*	0	*0*
Phosphate	Augelite	2.17	*0.32*	0	*0*	1.1	*0.31*	0	*0*
	Metavariscite	0	*0*	0	*0*	0.95	*0.36*	3.24	*0.35*
	Σ	2.17	*0.32*	0	*0*	2.05	*0.48*	3.24	*0.35*
Gibbsite		1.51	*0.29*	2.92	*0.28*	3.05	*0.31*	2.53	*0.31*
Goethite		1.47	*0.2*	1.35	*0.18*	2.11	*0.2*	1.65	*0.18*
Feldspar	Orthhoclase	0.46	*0.26*	2.23	*0.31*	1.27	*0.2*	7.95	*0.44*
	Albite	6.38	*0.34*	6.14	*0.34*	2.77	*0.41*	5.73	*0.34*
	Σ	6.84	*0.43*	8.37	*0.46*	4.04	*0.46*	13.68	*0.56*
Clays	Dickite	3.57	*0.59*	0	*0*	6.32	*0.7*	1.86	*0.54*
	Haolloysite	3.05	*0.44*	2.62	*0.38*	3.92	*0.57*	3.48	*0.4*
	Kaolinite	10.43	*0.9*	2.94	*0.37*	9.27	*0.88*	2.68	*0.69*
	Nacrite	0.79	*0.5*	1.14	*0.31*	7.82	*0.95*	0	*0*
	Σ	17.84	*1.26*	6.7	*0.61*	27.33	*1.58*	8.02	*0.96*
Quartz		68.5	*0.64*	77.76	*0.67*	59.38	*0.6*	68.72	*0.68*
Tsargorodtsevite		0	*0*	0	*0*	0	*0*	0	*0*
Vermiculite		0	*0*	0	*0*	0	*0*	0	*0*
Melanovanadite		1.17	*0.21*	1.98	*0.21*	0	*0*	2.13	*0.24*
Σ		99.5	*1.57*	99.99	*1.12*	99.98	*1.88*	99.97	*1.42*

Table 2. Summary of the mineral average content of samples used in this study based on their bedrock type and topographic position.

		Oxisols	Ox Ridge	Ox Valley	Dystrudepts	Dys Ridge	Dys Valley
Elevation(m)		657	660	653	653	666	640
Apophylite		0.93	0.75	1.1	1.1	1.24	0.96
Phosphate	Augelite	6.02	5.74	6.3	1.46	1.63	1.29
	Metavariscite	4.86	5.14	4.58	2.23	2.02	2.44
	Total Phosphate	10.88	10.88	10.88	3.69	3.65	3.73
Gibbsite		6.16	3.39	8.93	3.01	1.53	4.5
Goethite		6.61	7.21	6	2.63	2.89	2.37
Feldspar	Orthhoclase	4.25	4	4.5	3.36	2.74	3.98
	Albite	0	0	0	11.06	10.58	11.53
	Σ	4.25	4	4.5	14.41	13.32	15.51
Clays	Dickite	10.97	8.84	13.1	3.64	4.93	2.35
	haolloysite	14.82	17.56	11.99	5.03	5.81	4.24
	Kaolinite	14.82	16.82	12.82	8.27	10.8	5.75
	Nacrite	11.41	12.38	10.44	4	6.75	1.25
	Σ	52.02	55.69	48.35	20.94	28.29	13.59
Quartz		17.84	16.45	19.23	52.35	47.19	57.51
Tsargorodtsevite		1.3	1.61	0.99	0.55	0.73	0.36
Vermiculite		0	0	0	0.27	0.27	0.27
Melanovanadite		0	0	0	0.97	0.77	1.17
Σ		99.99	99.98	99.98	99.92	99.88	99.97

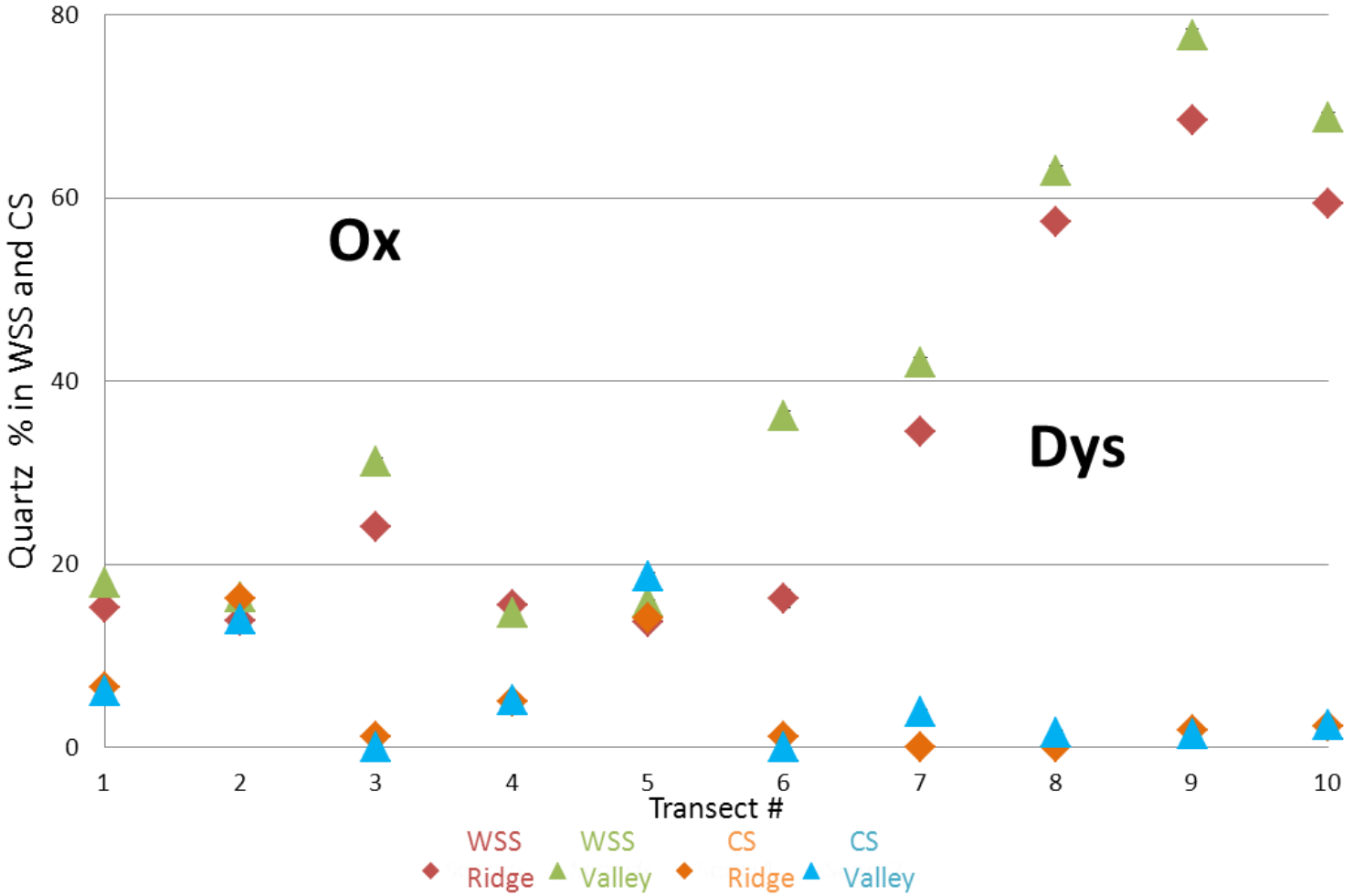

Figure 10. Percentage of quartz in 0-20cm whole soil samples and clay size fractions in Ox and Dys soils

What of a note here is that orthoclase and albite are considered together as feldspar. Albite found in samples from Dystrudepts sites reflects the low weathering degree raletived to the Oxisols.

The relationship between the total clay and the change of elevation and two different bed rock types are shown in Figure 11. The total clay percentage shows distinct difference between the two bedrock types. Also it is clear that the soil samples from high elevation (henceforth will be called ridge) have higher total clay content than the samples from lower elevation (henceforth will called valley). On the other hand, gibbsite show the opposite relationship to that of clay as shown in Figure 12.

The higher total clay content in ridges in contrast to valleys can be explained: 1) more feldspar was weathered to clays in the ridges than in the valleys, 2) the clay-minerals in the valley were more weathered to gibbsite than soil samples in the ridge.

Possibility one above is based on the hydrolyses of feldspar weathering to clays according on the equation

$$\underset{\text{orthoclase}}{2\ KAlSi_3O_8} + 2\ H^+ + 9\ H_2O \rightarrow \underset{\text{kaolinite}}{AlSi_2O_5(OH)_2} + 4\ \underset{\text{dissolved silica}}{H_4SiO_4^0} + 2\ K^+$$

So when all other factors being equal, the data should show less feldspar content in the ridge than in the valley. However, the data are near equal amount (within analytical uncertainty) of feldspar in valley and ridge samples in the two bedrock sites as show in Figure 13.

Explanation two above based on the equation

$$\underset{\text{kaolinite}}{AlSi_2O_5(OH)_2} + 5\ H_2O \rightarrow 2\ \underset{\text{gibbsite}}{Al(OH)_3} + 2\ H_4SiO_4^0$$

This means because of the higher weathering and leaching, which could interpreted as due to the closeness of the valley soils to water table, the gibbsite content in the valley should higher than in the ridge. This possibility is supported by the

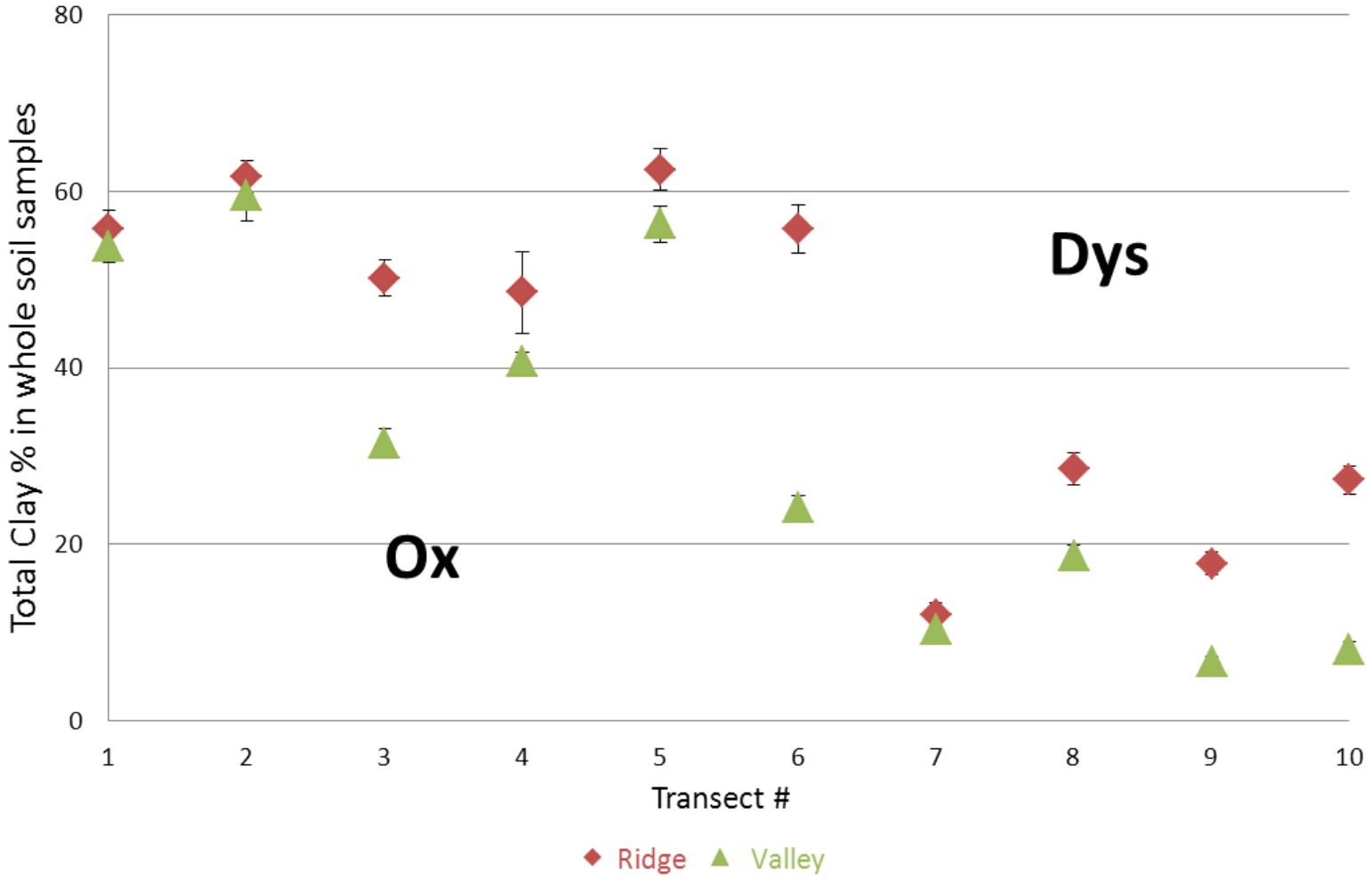

Figure 11. Total Clay percentage in 0-20cm whole soil samples in Ox and Dys soils

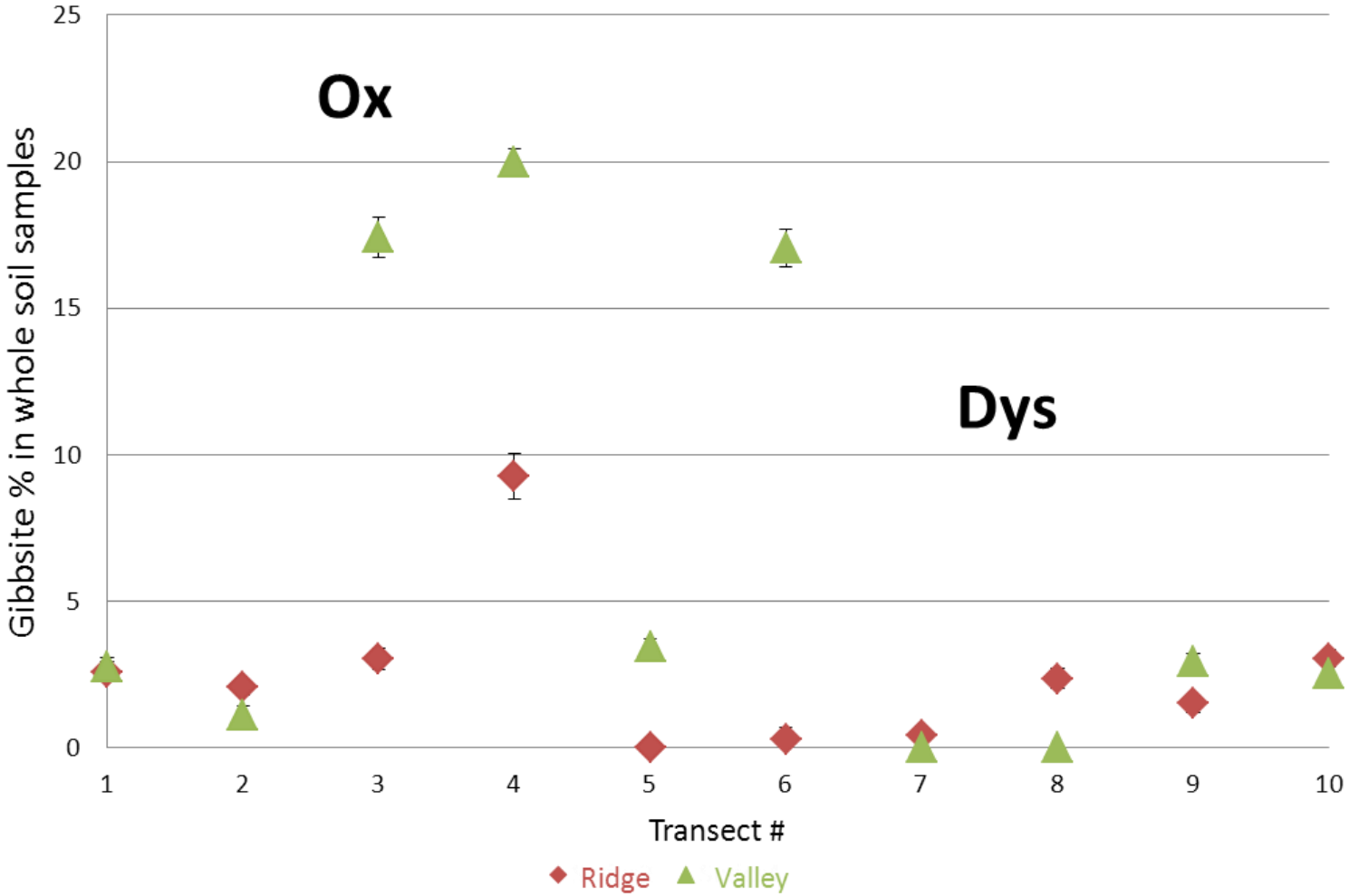

Figure 12. Percentage of gibbsite in 0-20cm whole soil samples in Ox and Dys soils

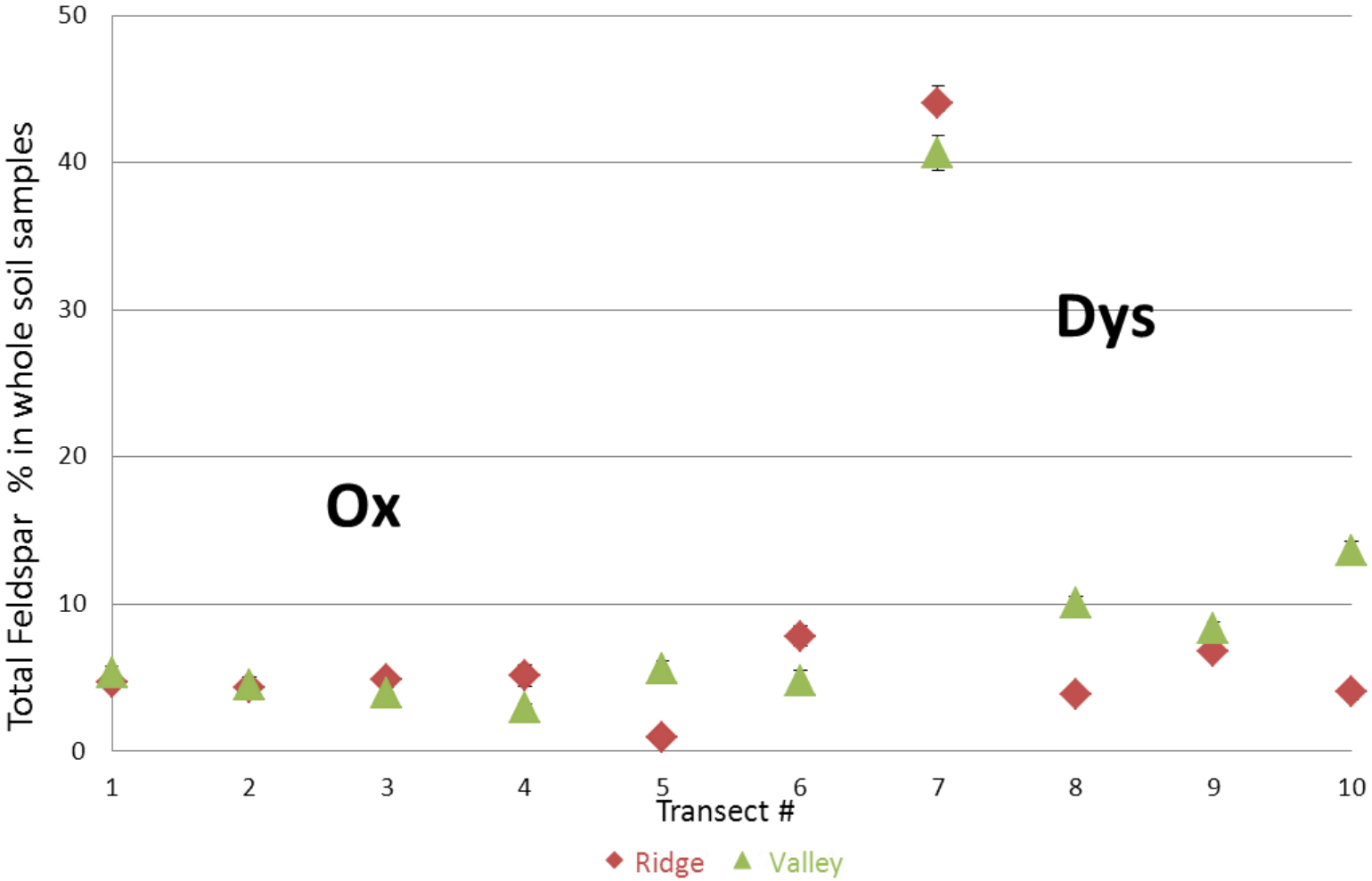

Figure 13. Percentage of total feldspars in 0-20cm whole soil samples in Ox and Dys soils

high concentration of gibbsite in valley soil sample than samples from ridge as mentioned above and shown in Figure 12. These patterns of the amount of total clays, feldspars, and gibbsite within each and between transects, in combination with Equations above, indicate that soil in the valleys are more weathered than soil from.

The presence of iron oxides and hydroxides (e.g. goethite) and organic matter in the analyzed soil samples cause the scatter of the diffracted x-ray beam. Therefore, the removal of these compounds greatly enhance the parallel orientation of clay crystals and hence brings out some x-ray diffraction peaks that are otherwise difficult or impossible to detect. To test the magnitude of that effect in the XRD patterns obtained, one sample was treated for the removal of iron oxides and hydroxides and organic matter. The clay-size fraction of sample number Col Ox 1-4 (6.96% goethite) was chosen for that treatment. First, sample was treated by hydrogen peroxide to remove organic matter. Then iron oxides and hydroxides were removed by a dithionite-citrated system buffered with sodium bicarbonate. (Mehra and Jackson, 1960)

The XRD pattern of the treated sample didn't show significant improvement as to the clarity and the number of peaks present in the XRD profile. However, compared with the untreated sample, the treated sample does not show the peak at 14° 2θ. (Figure 14)

By further analysis, two minerals are found to account for the presence of the ~14°2θ. These two minerals are Metavarscite (14.048°2θ, Intensity 48.8%) and tsaregorodtsevite (13.979°2θ, Intensity 60%).

As shown in Table 1, the percentage of tsaregorodtsevite is range from 0 to 4 in whole soil samples and from 0 to 6 in clay-size fractions. Generally, the samples from Oxisols sites contain more tsaregorodtsevite than in samples from Dys sites. Also, in the same transect the tsaregorodtsevite is always high in the ridge than in the valley.(Figure 15)

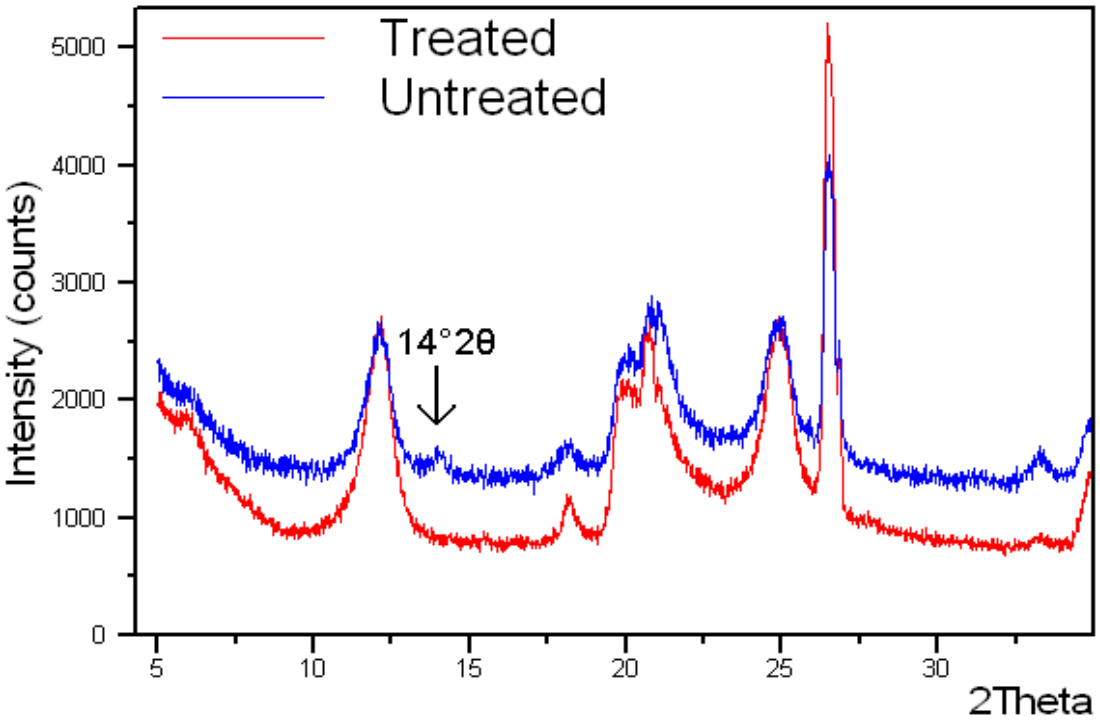

Figure 14. XRD patterns of treated and untreated clay-size fraction of sample # Col Ox 1-4. See text for details.

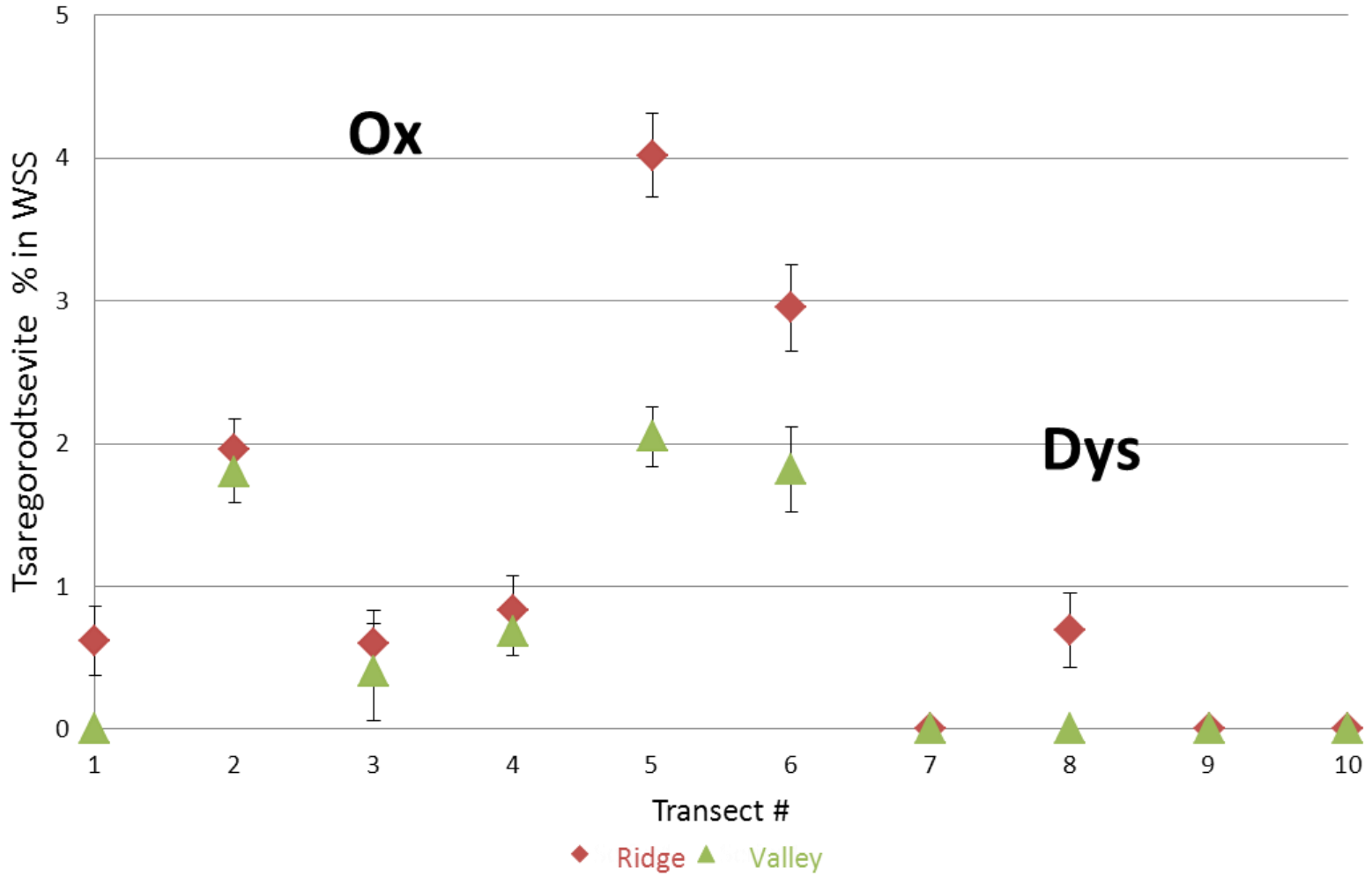

Figure 15. Percentage of tsargorodtsevite in 0-20cm whole soil samples in Ox and Dys soils

According to Dana's classification of minerals the mineral tsaregorodtsevite ($N(CH_3)_4AlSi_5O_{12}$) is listed as a tectosilicate of the feldspathoid mineral group. (C. Klein, B. dutrow, 2007.) It contains 6.22% aluminum, 32.39% silicon, 2.79% hydrogen, 11.08% carbon, 3.23% nitrogen and 44.28% oxygen (Jambor, Roberts, and Vanko, 1994). The nitrogen and carbon ions are present in the mineral in the form of organic cation Tetramethylammonium (TMA), with net charge $+1[N(CH_3)_4]^{1+}$. Detailed crystal structure (Figure 16) of tsaregorodtsevite illustrates that the TMA organic cation occupy the empty channels and cages created by the framework of SiO_4 tetrahedra. (Vahedi-Faridi, Guggenheim, 1997)

It is important to note that the presence of that mineral in the soil samples studied must be confirmed by further investigations. If the presence of that mineral in the soil is confirmed, it can provide a low energy mechanism for the sequestration of carbon and nitrogen in tropical soils as the forests in Puerto Rico.

Rietveld best-fit profiles for samples studied indicate the present of two phosphate minerals; augelite ($Al_4(PO_4)_3(OH)_3$) and metavariscite ($AlPO_4{\cdot}2H_2O$). As indicate by the chemical formula of this two minerals it is clear that augelite is the dehydrate form of metavariscite. The occurrence of metavariscite is largely restricted to soils and aluminous rocks like Al-rich igneous rocks and shales, which interacted with P-rich hydrothermal solutions or groundwater. Metavariscite dehydrates to berlinite ($AlPO_4$) and a hydrous P-Al-rich fluid. This dehydration reaction $AlPO_4{\cdot}2H_2O \rightarrow AlPO_4 + 2H_2O$ is metastable, at low concentrations of P in the fluid, because berlinite breaks down at lower temperature to augelite $Al_4(PO_4)_3(OH)_3 + H_3PO_4 + H_2O$. (K.Drüppel, A. Hösch and G. Franz, 2007)

All samples studied except Col Dys 6-132 contain phosphate minerals (augelite and metacariscite) with the total percentage up to 15%. Augelite is the dominant phosphates present in all the samples (Figure 17). Metavariscite has the small percentage from 1 to 6 (Figure 18). The total amount of the two minerals is shown in Figure 19 which shows no relationship between the ridge and valley.

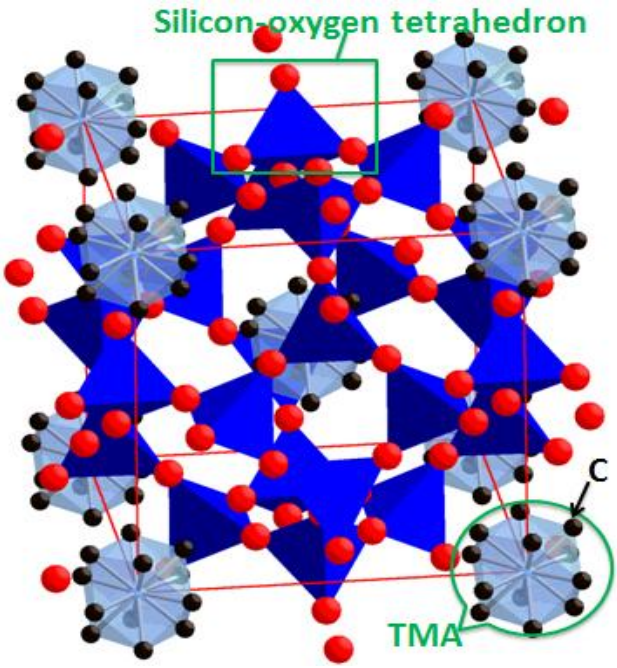

Figure 16. Crystal structure of tsaregordtsevite (Jambor, et. al., 1994)

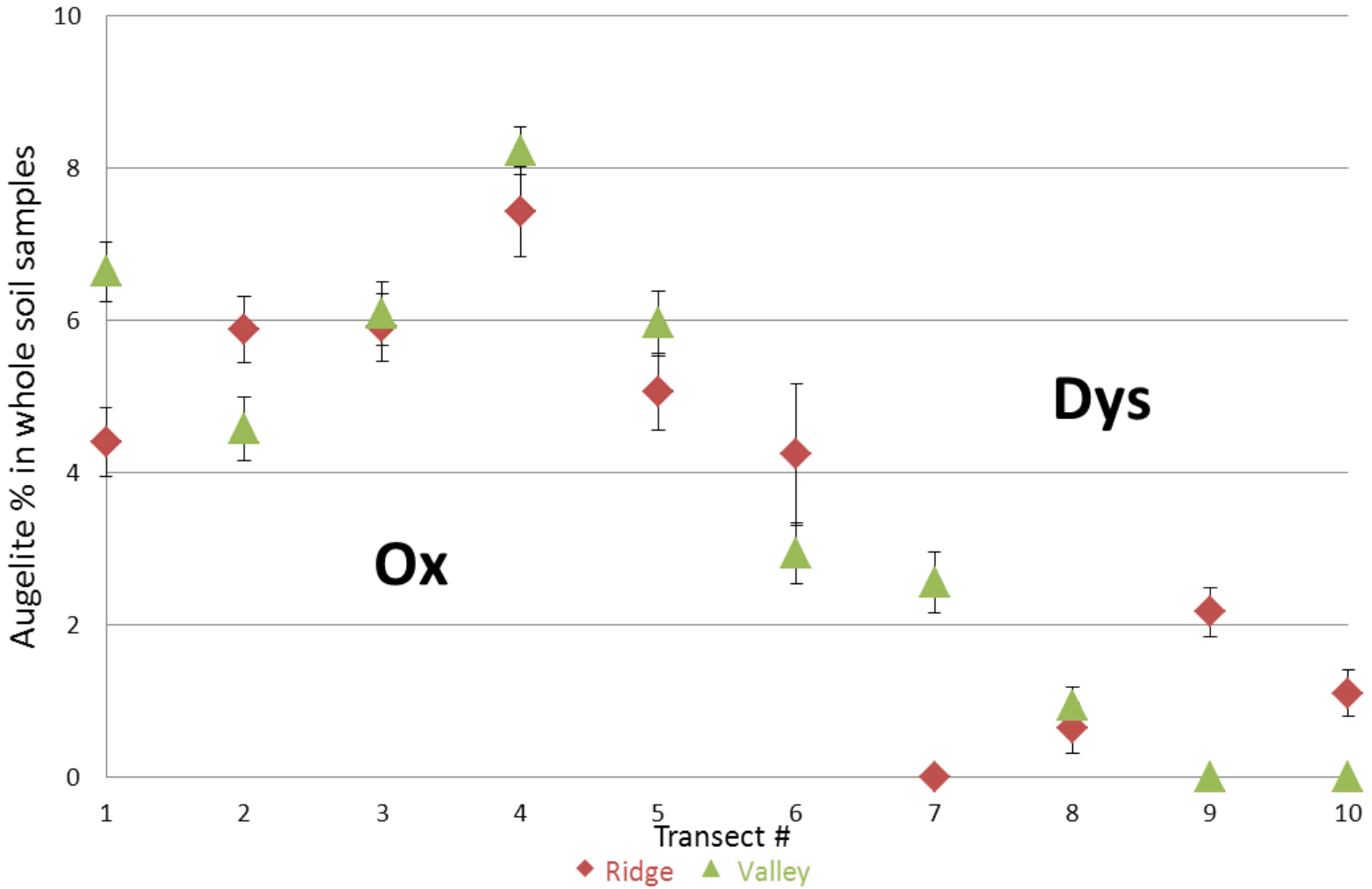

Figure 17. Percentage of augelite (phosphate mineral) in 0-20cm whole soil samples in Ox and Dys soils

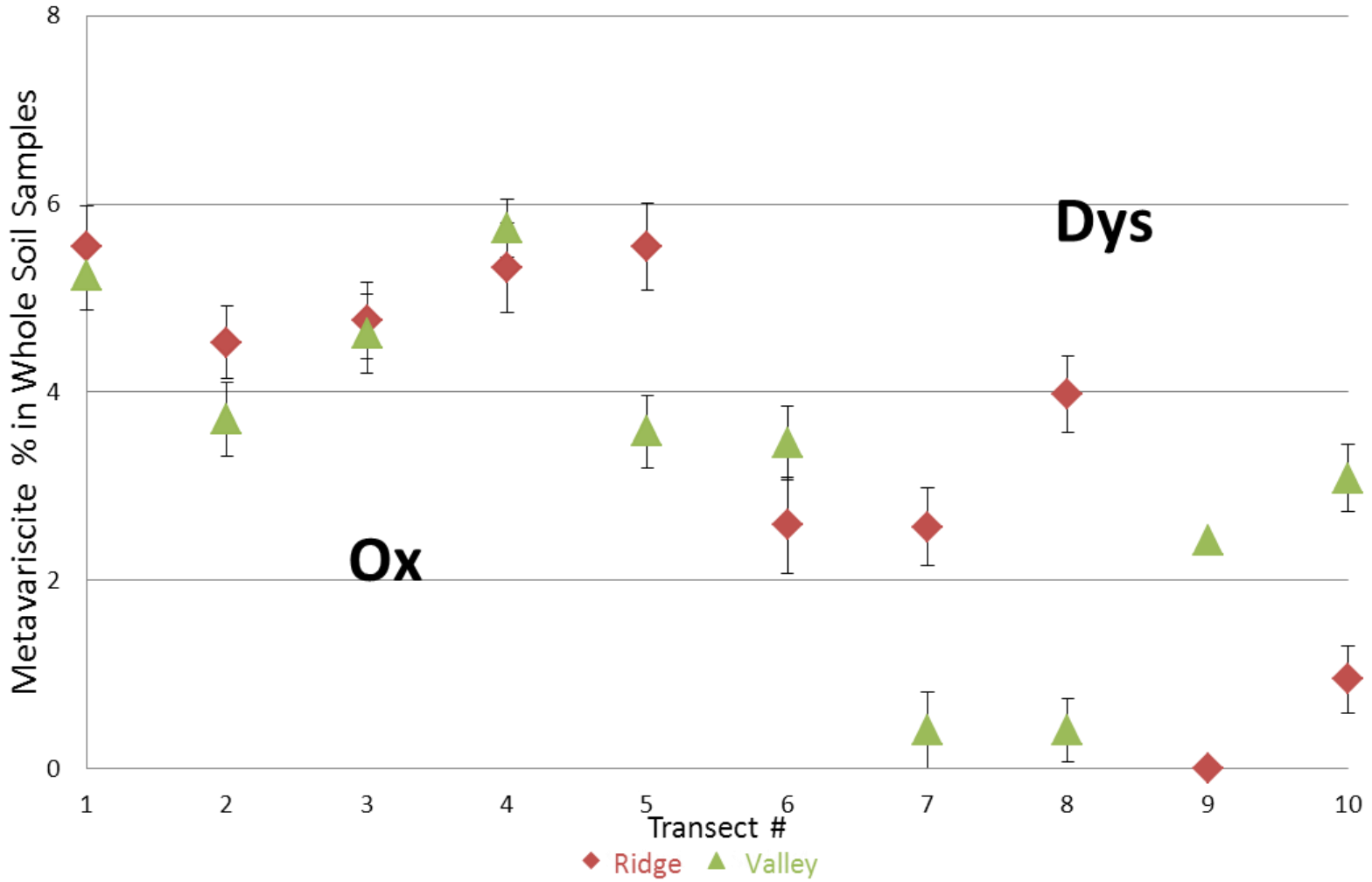

Figure 18. Percentage of metavariscite (phosphate mineral) in 0-20cm whole soil samples in Ox and Dys soils

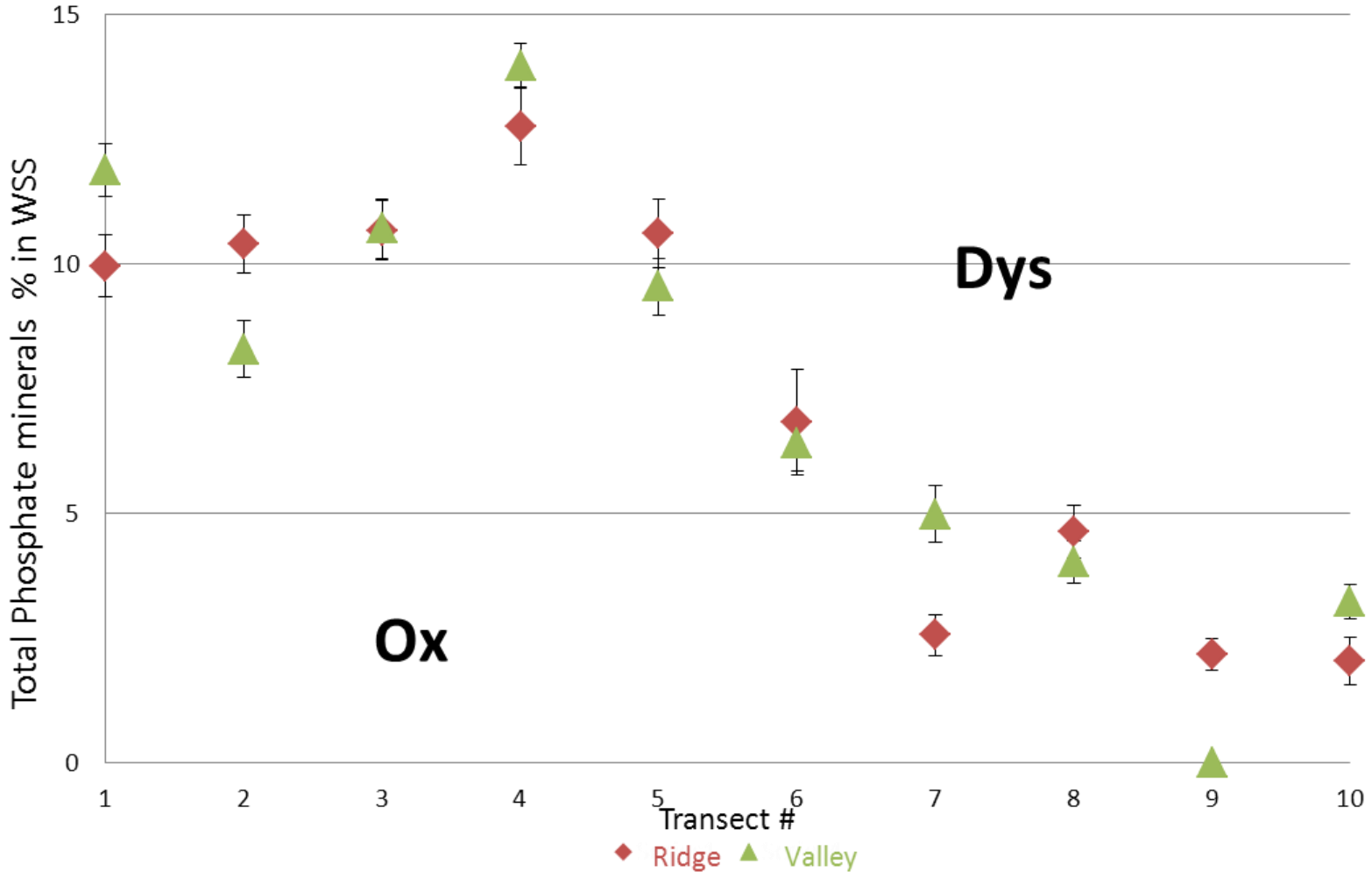

Figure 19. Percentage of total phosphate minerals in 0-20cm whole soil samples in Ox and Dys soils

The diagrams show that whole soil samples from the Oxisols sites have higher concentration of the two phosphate minerals than samples from the Dystrudepts site. This pattern most probably is due to the attachment of the phosphate minerals to clay mineral surfaces. This hypothesis is supported by the fact that there are more clays present in the Oxisols site than in the Dystrudepts site as mentioned above in figure 9. The lack of difference of total clay and total phosphate minerals in the clay-size fraction (Figure 20 and 21) between Oxisols and Dystrudepts provide further evidence for this hypothesis. Further study(s) must be carried out to investigate the nature of the association of clay and phosphate minerals.

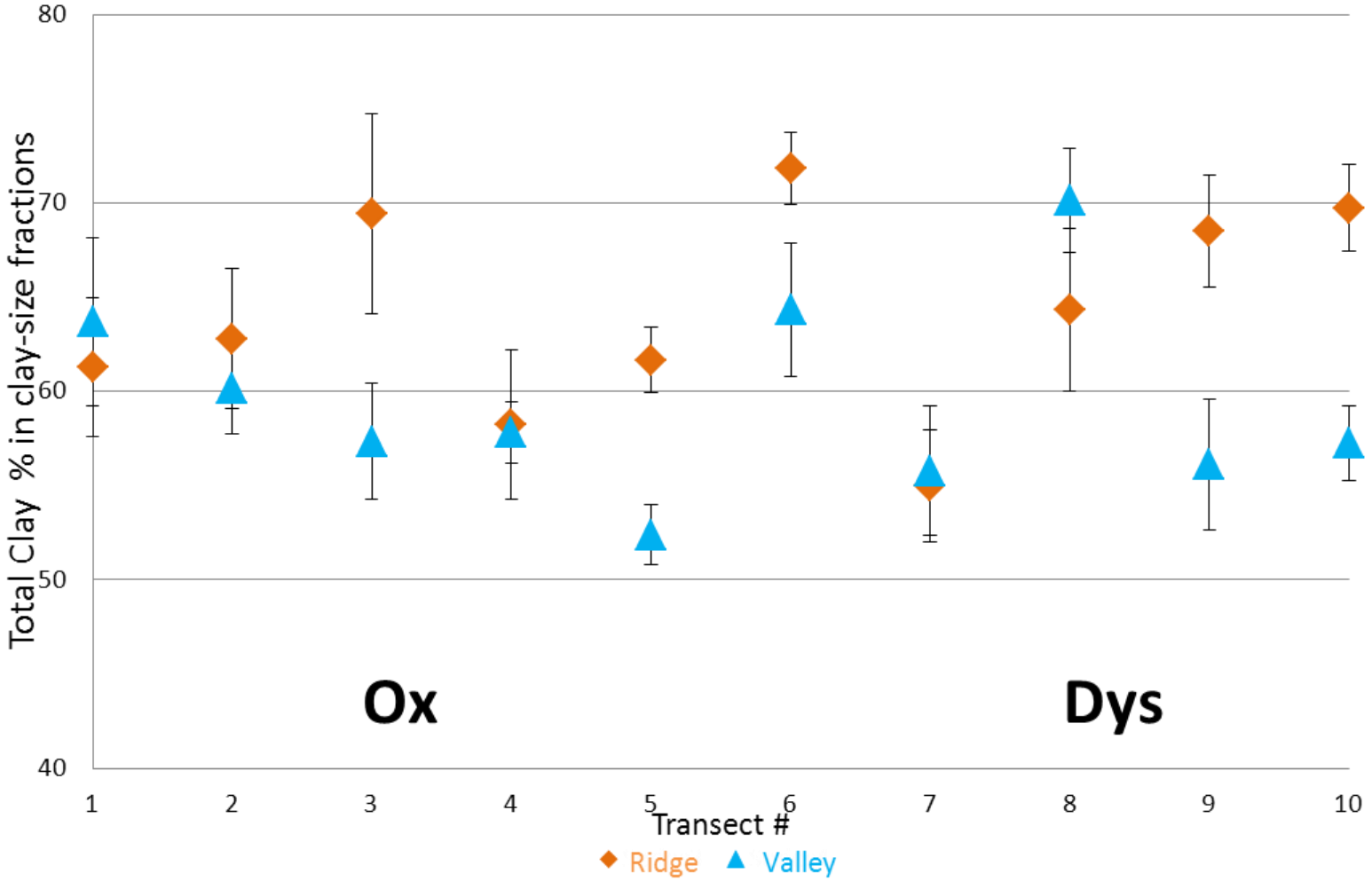

Figure 20. Percentage of total clay minerals in 0-20cm clay-size fractions in Ox and Dys soils

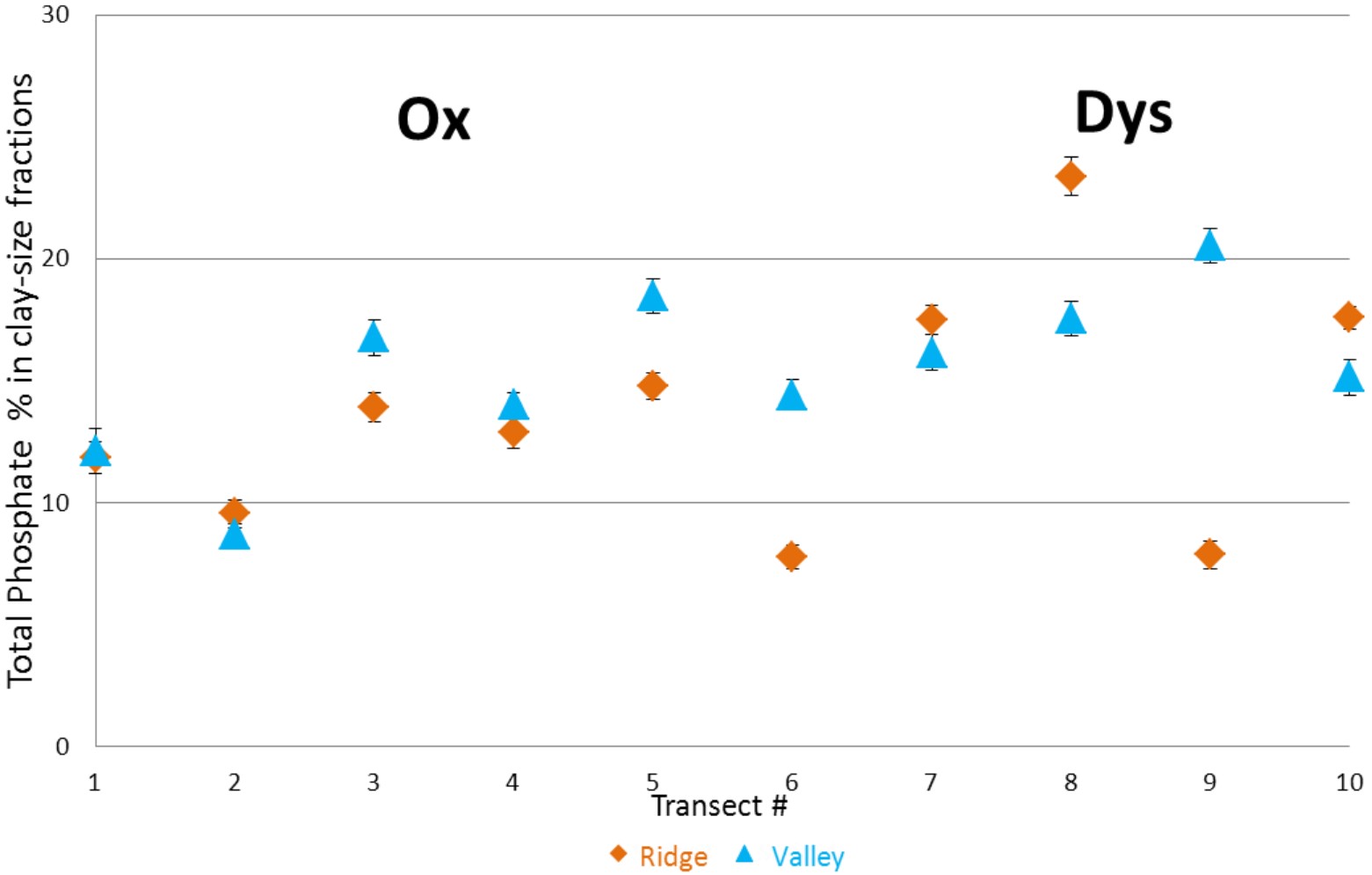

Figure 21. Percentage of total phosphate minerals in 0-20cm clay-size fractions in Ox and Dys soils

Conclusions

1. Soil sample from Oxisols (Volcanclastic bedrock) sites contain higher percentage of clay minerals than the samples from Dystrudepts (Quartz-diorite bedrock) sites.

2. The general pattern of the percentage of total clays, feldspars, and gibbsite within each and between transects indicate that soil in the valleys are more weathered than the soil from ridges which could interpreted as due to the closeness of the valley soils to the water table.

3. Phosphate minerals present in the soil are augelite and metacariscite. The whole soil samples from the Oxisols sites have higher concentration of the two phosphate minerals than the samples from the Dystrudepts sites. This pattern is most probably due to the attachment of the phosphate minerals to clay mineral surfaces.

4. Tsaregorodtsevite was detected in almost all the Ox samples and few Dys samples. The presence of the organic cation Tetramethylammonium in the cavities between the oxygen-silicon tetrahedra of the tsaregorodtsevite structure is consistent with a low energy mechanism for the sequestration of carbon and nitrogen in tropical soils. However, the chemical and thermodynamic details of this mechanism need to be worked out by further investigation.

References

Bailey, S. W., (1963) Polymorphism of the kaolin minerals, American mineralogist, vol 48: 1196-1209.

Bayliss, P., and Hughes, J.M., (1985) X-ray diffraction data for melanovanadite. Amer. Mineral., vol. 70: 644–645.

Blatt, H., Tracy, R. J. and Owens, B. E. (2006) Weathering and Soils. Petrology*, 3rd edition*: 232-243.

Breemen, N., Buurman, P. (2002) Soil Formation, Second edition.

Cruz,() Maria Dolores Ruiz. Genesis and evolution of the kaolin-group minerals during the diagenesis and the beginning of metamorphism.

Gee, G. W., Bauder, J. W. (1986)Particle-size Analysis, Methods of Soil Analysis, Part 1. Physical and Mineralogical Methods-Agronomy Monograph no.9, 2nd Edition: 383-409.

Jambor, J. L., Roberts, A. C., and Vanko, D. A., (1994) New mineral names, America mineralogist, vol 79: 1009-1014.

Kesler, S.E., Sutter, J.F. (1979) Chemical analysis of intrusive rocks from Puerto Rico.

Kirsten Drüppel, Andreas Hösch and Gerhard Franz, (2007) The system Al_2O_3-P_2O_5-H_2O at temperatures below 200 °C: Experimental data on the stability of variscite and metavariscite $AlPO_4 \cdot 2H_2O$. *American Mineralogist*; vol. 92: 1695-1703

Klein, C., Dutrow, B. (2007) The manual of mineral science, 23rd edition.

McKnight, T.L., Hess, D. (2000) Climate Zones and Types: The Köppen System"

Mehra, O. P., and Jackson, M. L., (1960) Iron oxide removal from soils and clays by a dithionite-citrate system buffered with sodium bicarbonate. Clays & Clay Miner, vol 7:317-327.

Murray, H. H., (1988) Kaolin minerals: Structures and Stabilities, Reviews in mineralogy, vol. 19: 29-66.

USDA, NRCS, 2001. Soil Survey of Caribbean National Forest and Luquillo Experimental, commonwealth of Puerto Rico.

Us Forest Service (2009) El Yunque National Forest

USGS open file Report 01-041.

Vahedi-Faridi, A., Guggenheim, S., (1997) Crystal Structure of Tetramethylammonium-exchanged Vermiculite, Clay and Clay minerals, vol 45: 859-866.